Article

Not peer-reviewed version

# Energy-Efficient Routing Protocols for IoT-Based Wireless Sensor Networks in Nuclear Facility Monitoring

Mohamed S. El Tokhy , Ibraheem Mahmoud Fayed * , Elsayed H. Ali *

Posted Date: 18 March 2026

doi: 10.20944/preprints202603.1394.v1

Keywords: wireless sensor networks; power consumption optimization; radioactive environment monitoring; LPWAN; data aggregation; battery management; routing protocols

 doi:10.20944/preprints202603.1394.v1



*Article*

# Energy-Efficient Routing Protocols for IoT-Based Wireless Sensor Networks in Nuclear Facility Monitoring

**Mohamed S. El Tokhy [1], Ibraheem Mahmoud Fayed [2,*] and Elsayed H. Ali [3,*]**

[1] Joint Institute for Nuclear Research, Dubna, Moscow 141980, Russian Federation
[2] National Telecommunication Institute, Cairo, Egypt
[3] Engineering Department, NRC, Egyptian Atomic Energy Authority, Cairo, Egypt
* Correspondence: ibrahim.fayed@nti.sci.eg (I.M.F.); sayedmahdy@yahoo.com (E.H.A.)

**Abstract**

Reliable and energy-efficient wireless sensor networks (WSNs) are essential for continuous monitoring in nuclear facilities, where harsh environmental conditions, limited battery resources, and strict safety requirements demand robust communication performance. This study presents a comparative evaluation of four energy-efficient routing protocols -Low-Energy Adaptive Clustering Hierarchy (LEACH), Power-Efficient and Balanced Aggregation in Sensor Networks (PEBAIS), Threshold-sensitive Energy Efficient Network (TEEN), and Geographic Adaptive Fidelity (GAF)-for IoT-based monitoring applications in radioactive environments. Simulation experiments were conducted using 200 sensor nodes over ten communication rounds within a 5000 $m^2$ monitoring area. The network was initialized with a node energy of 0.5 J, a packet size of 4000 bits, and an energy consumption model of $50 \times 10^{-9}$ J/bit. The protocols were assessed in terms of energy consumption, network lifetime, latency, throughput, signal-to-noise ratio (SNR), and bit error rate (BER). The results demonstrate distinct operational advantages among the evaluated protocols. LEACH provided efficient clustering and data aggregation but exhibited notable variations in latency and residual energy, which limited long-term stability. PEBAIS achieved the most balanced overall performance, maintaining low energy consumption, stable throughput, and zero BER, despite moderate SNR fluctuations. TEEN showed strong suitability for event-driven nuclear monitoring by reducing unnecessary transmissions and providing rapid response to critical changes, although its performance depended strongly on threshold configuration. GAF significantly extended network lifetime by deactivating redundant nodes, but its reliance on geographic scheduling introduced delays in time-sensitive applications. Overall, PEBAIS and GAF proved most effective for sustained monitoring, while TEEN was particularly suitable for urgent event detection scenarios. The findings highlight the importance of protocol selection in designing reliable IoT-enabled WSNs for nuclear facility monitoring and support the development of future hybrid routing frameworks that combine energy efficiency, responsiveness, and operational reliability in hazardous environments.

**Keywords:** wireless sensor networks; power consumption optimization; radioactive environment monitoring; LPWAN; data aggregation; battery management; routing protocols

---

## 1. Introduction

Monitoring radioactive environments is essential to safeguard public health and mitigate the hazards of radiation exposure. Wireless Sensor Networks (WSNs) present a viable solution for real-time, continuous monitoring of these high-risk areas [1–3]. These systems comprise spatially distributed sensor nodes that collaboratively gather and relay data to a central base station. However,

 doi:10.20944/preprints202603.1394.v1



their performance is often limited by the finite battery power of sensor nodes, making it crucial to develop energy-efficient strategies to extend their operational lifespan. Clustering Algorithms and Energy Efficiency [4–6]. Clustering techniques have become a prominent approach to reducing energy consumption in WSNs. A prime example is the Low-Energy Adaptive Clustering Hierarchy (LEACH), which demonstrates the benefits of cluster-based communication by periodically rotating the role of cluster heads among nodes, thereby lowering energy overhead. Enhanced versions like the Energy Efficient Unequal Multilevel Clustering (EEUMC) further optimize energy usage by considering factors such as residual energy and distance to sink nodes, effectively reducing redundant transmissions and improving network longevity[7,8]. Advanced clustering techniques also incorporate game-theory-based methods, dynamically selecting cluster heads to balance energy consumption and ensure equitable load distribution. For instance, EDRP-GTDQN employs game theory integrated with deep reinforcement learning (DRL) to optimize cluster head selection based on energy levels and network topology[1,9,10]. These strategies enhance scalability and energy efficiency in large-scale WSN deployments. Routing protocols in WSNs face unique obstacles in radioactive settings, such as high interference, radiation, and restricted accessibility. Gradient-based routing protocols, including Directed Diffusion and Ubiquitous Mobile Gradient (UMG), address these challenges by optimizing data aggregation and minimizing redundant communication, which reduces energy expenditure [11,12]. Modern enhancements incorporate mobility detection and in-network data processing, improving adaptability and efficiency. In extreme conditions, methods like acoustic communication and adaptive clustering are vital for reliable functionality. For example, the Energy-Efficient Routing Protocol based on Layers and Unequal Clusters (EERBLC) adjusts cluster sizes and routing paths dynamically to prevent energy imbalances and mitigate “hotspots.” Hybrid models combining clustering and multi-hop communication further enhance energy efficiency and system resilience [13,14]. Reinforcement Learning (RL) has revolutionized routing and energy optimization strategies in WSNs. RL-based protocols excel over traditional methods by dynamically learning optimal routing paths based on real-time environmental factors [15]. For example, Zhang et al. proposed an RL-driven multi-hop routing protocol that considers variables such as the number of hops, residual energy, and buffer size to optimize data transmission. Similarly, hierarchical routing protocols leveraging Q-learning, like FTIEE, prioritize relay node selection based on energy efficiency and distance, leading to significant energy savings[16–18]. Recent advancements integrate RL with deep learning technologies, such as Deep Q-Networks (DQN), to optimize routing in complex, large-scale networks[1,19]. These systems employ neural networks to dynamically refine routing strategies, ensuring a balance between energy consumption and communication delays. Notably, EDRP-GTDQN combines game theory with DQN to optimize cluster head selection and multi-hop routing, addressing challenges like high node density and frequent topology changes, thereby enhancing network performance and reliability. WSN deployment in nuclear facilities faces unique challenges, including radiation interference and the requirement for uninterrupted, resilient operation [20]. Innovations such as LoRa-based low-power communication protocols and adaptive energy-harvesting mechanisms have been instrumental in meeting these demands. Specialized protocols designed for event detection and fault tolerance in radiation-intensive environments often use bio-inspired algorithms and wake-up radio technologies to minimize idle energy consumption. These techniques not only boost the resilience of WSNs but also ensure consistent and reliable data transmission under extreme conditions, making them suitable for monitoring critical parameters in hazardous nuclear environments. Such advancements pave the way for safer and more efficient radiation monitoring systems, protecting both human and environmental health. WSN have emerged as versatile, scalable, and cost-effective solutions for controlled supervision across various infrastructures. Comprising small, low-power sensor nodes capable of processing and wirelessly transmitting data, these nodes -referred to as motes- are deployed in diverse environments to support applications such as smart grids, industrial and home automation, military surveillance, and habitat monitoring [21]. Innovations in electronic circuit design have resulted in lighter, cheaper, and more energy-efficient sensors. However, energy efficiency remains a key research focus [22]. Motes in many applications rely on non-rechargeable batteries, limiting the network's lifespan [23]. Network lifetime is often defined by the time until the first mote fails, the time until a certain fraction of motes fail, or the time until all motes are non-functional [6,10,24]. Network efficiency starts to degrade with the failure of the first mote, highlighting the need to optimize connectivity, coverage, and node longevity. Although sustainable energy sources have been explored, effectively managing available energy is crucial to extending network operation [25]. WSNs monitor parameters such as location, humidity, or temperature, depending on the application. These parameters are often interdependent, necessitating data aggregation from neighboring sensors to conserve energy [26]. Since data processing consumes significantly more energy than transmission, compressing data before communication is vital. This approach reduces energy consumption, extends network lifetime, and improves communication efficiency [27]. Direct data transmission from individual nodes to the base station, however, accelerates energy depletion and risks network failure when motes exhaust their power [28]. Energy constraints in motes pose a significant challenge for WSNs. Unlike traditional wireless networks, WSNs demand strategies for optimal energy utilization [28]. Grouping motes into clusters has been shown to enhance energy efficiency and scalability. Each cluster designates a Cluster Head (CH) to communicate with other CHs and the sink node, reducing energy requirements for direct transmissions [29]. Routing protocols play a critical role in clustering by determining optimal paths between CHs and the sink to further minimize energy consumption [30]. Routing protocols offer advantages such as scalability, data aggregation, reliability, and fault tolerance [31]. Many studies employ heuristic and meta-heuristic algorithms to select CHs, improving network reliability and energy efficiency. These methods have demonstrated success in extending the operational lifespan and reliability of WSNs [21]. By addressing challenges related to energy optimization, clustering, and routing, WSNs can be tailored to meet the diverse demands of various applications. Power consumption is a critical challenge in WSNs, as sensor nodes typically rely on constrained, non-replaceable power sources[32]. The depletion of energy can disrupt monitoring operations, particularly in scenarios where uninterrupted functionality is crucial for safety. In nuclear facilities, where nodes are exposed to high levels of radiation and electromagnetic interference, achieving energy efficiency while maintaining robust communication protocols is essential. This necessitates advanced optimization techniques that not only conserve power but also improve the resilience and adaptability of WSNs[12]. Recent advancements in IoT frameworks have introduced innovative strategies to address energy constraints in WSNs [32]. These include: Reducing the active time of sensor nodes to conserve power while maintaining data accuracy[33]. Employing protocols that select optimal paths based on energy metrics to distribute power consumption evenly across the network[15]. Utilizing techniques like dynamic cluster head rotation to balance energy usage among nodes, minimizing energy overhead. Leveraging environmental energy sources, such as solar or kinetic energy, to recharge sensor nodes and extend network lifetime[34]. Integrating machine learning and bio-inspired algorithms has significantly enhanced the capability of WSNs to manage power dynamically while adapting to environmental fluctuations[23,35]. Machine learning algorithms, such as reinforcement learning, enable nodes to learn from their surroundings and make real-time adjustments to routing and power strategies. Bio-inspired techniques, modeled on natural processes like swarm intelligence, provide decentralized and scalable solutions for energy optimization[15,36]. In nuclear facilities, where operational reliability and sensor lifespan are critical, these energy optimization methods are invaluable[37–39]. They ensure consistent and dependable data transmission, even in the presence of extreme radiation and interference. Advanced optimization frameworks combining IoT, machine learning, and adaptive protocols address the dual requirements of energy efficiency and robust performance, making them integral to the safe and efficient operation of monitoring systems in such challenging environments [40]. Routing protocols are essential for optimizing energy efficiency and ensuring the performance of WSNs. The effectiveness of these protocols is particularly significant in contexts such as radioactive environment monitoring, where uninterrupted operation and power conservation are critical. Several well-studied protocols address these challenges through innovative approaches to routing and energy

Preprints.org (www.preprints.org) | NOT PEER-REVIEWED | Posted: 18 March 2026 doi:10.20944/preprints202603.1394.v1



management. LEACH reduces energy consumption by rotating cluster head roles among nodes, distributing energy load evenly across the network. This approach minimizes node depletion and extends network lifespan [21]. TEEN Proposed by [41], TEEN is tailored for time-critical applications. It uses thresholds for sensed data to reduce unnecessary transmissions, conserving energy while ensuring timely responses. Power-Efficient Gathering in Sensor Information Systems (PEGASIS) Developed by [42], PEGASIS arranges nodes into chains, with each node transmitting data to its nearest neighbor. This strategy minimizes long-distance transmissions, further reducing energy consumption. Power-Efficient and Balanced Aggregation in Sensor Networks (PEBAIS ) PEBAIS focuses on balancing energy usage across all nodes by optimizing data aggregation[43]. This prevents specific nodes from depleting their energy prematurely, thus improving network longevity. Geographic Adaptive Fidelity (GAF) Proposed by [44,45], GAF reduces energy consumption by identifying and deactivating redundant nodes within each grid section. By ensuring that only essential nodes remain active, GAF maintains network fidelity while conserving power. This study aims to explore and optimize these protocols, tailoring them to the unique challenges of monitoring radioactive environments. Such settings demand not only energy-efficient operation but also resilience to interference and reliable data transmission. The study is embarked upon to ensure that different techniques of optimization are employed towards the optimal power consumption in WSNs used in monitoring radioactive environments. Details on sensor signals are to be generated and converted from analog to digital. Assess different protocols for low-power wide-area network LPWAN performance. Techniques for data aggregation and compression shall be realized, while designing battery management techniques that will extend the sensor nodes' lifetime. Apply and compare different routing protocols for the purpose of further optimizing communication paths with the goal of reducing energy consumption. The rest of the paper is organized as follows: Section 2 presents the methodology, which includes sensor signal generation, the LPWAN protocols, data aggregation and compression, battery management, and routing protocols. Section 3 presents results and discusses the various techniques applied and their performances. Section 4 does a critical comparative analysis of the routing protocols, while Section 5 summarizes the paper with detailed findings and possible future research.

## 2. Methodology

### *2.1. Signal Sensor Generation and Analog-to-Digital Conversion*

Sensor signals are generated to simulate the monitoring process. This plots typical sensor readings from sensors deployed in a radioactive environment. This is an important step because it lays the base for data processing or transmission over the network. A time vector is defined that will represent the duration of the monitoring process. It generates a single signal for each sensor, which can be a sine wave with different phase or frequency to simulate various sensor readings. It saves those analog signals, thus processed, in an Excel file. Then, it plots out the sensor readings against time. This enables an initial assessment of the signals that have been generated and ensures that, when working in a radioactive environment, the data will correctly describe the behaviour of a sensor in question. The next step involves the digitization of the analogue signals by applying one or another thresholding technique. One would compare the values of the analogue signal against a certain threshold value and assign it either 0 or 1, depending on whether it is below or above the threshold. This digital conversion necessary for data to be efficiently processed and transmitted within the WSN.

Figure 1 represents the analog and digital signals of five sensors over the period of 10 seconds. The left column analog signals are the sinusoidal waves added with random noise; this is representative of typical sensor readings in a radioactive environment. Above signals are digitized using a threshold value of 0 in the right column by taking values above the threshold as '1' and below as '0'. Digital signals reflect quite clearly the step function effect from such a thresholding process. This conversion would reduce the signals into simple transmissions within the WSN for efficient data manipulation, decrease the size of data to be sent, and conserve energy [46]. The effectiveness of this method in providing a clear, binary representation of the analogue data highlights its importance for optimizing power consumption and ensuring continuous, reliable monitoring in radioactive environments.

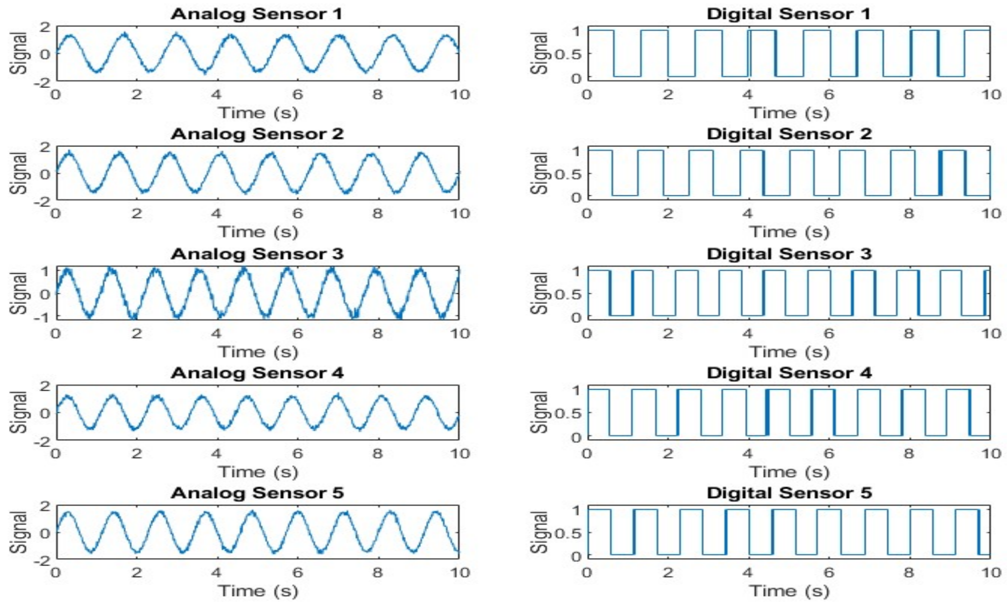


**Figure 1.** Analog and Digital Signal Representation of Sensors**.**

*2.2. Low Power Wide Area Network (LPWAN) Protocols*

The study evaluates the performance of three LPWAN protocols: LoRaWAN, SIGFOX, and VBIOT. These protocols are known for their ability to provide long-range communication with low power consumption, making them suitable for WSNs in radioactive environments[47].

2.2.1. Long Range Wide Area Network (LoRaWAN)

LoRaWAN is a protocol designed for wireless battery-operated devices in a regional, national, or global network. It features long-range communication, low power consumption, and secure data transmission. LoRaWAN operates in the unlicensed ISM (Industrial, Scientific, and Medical) bands, typically at frequencies around 868 MHz in Europe and 915 MHz in North America[12,26]. offers key features such as long-range communication capabilities, with distances ranging from 2-5 km in urban areas to 15 km or more in rural areas, and low power consumption, allowing devices to operate for several years on a single battery. The Adaptive Data Rate (ADR) optimizes data rate, time on air, and energy consumption, while AES-128 encryption ensures secure communication [48]. The LoRaWAN architecture includes End Devices (sensors or nodes that collect data), Gateways (which relay messages between end devices and the network server), the Network Server (which manages the network, filters duplicate messages, and handles adaptive data rates), and the Application Server (which processes and uses the data collected by the end devices). The physical layer of LoRa is based on Chirp Spread Spectrum (CSS) modulation, providing robustness against interference and multipath fading by using chirp signals where the frequency increases or decreases over time, spreading the signal over a wide frequency band and enhancing resilience to noise and interference[49]. Key LoRa modulation parameters include Bandwidth (BW), which determines the width of the chirp; Spreading Factor (SF), which represents the number of bits per symbol and ranges from 7-12; and Coding Rate (CR), which indicates the error correction capability and ranges from 4/5 to 4/8. The energy consumption of a LoRaWAN device is influenced by the transmission time (time-on-air), which depends on the data rate and the payload size[7,50]. The time-on-air ( $T_{air}$ ) can be calculated using:

$T_{air} = \frac{(P_{PL}+P_{HDR})\times 2^{SF}}{BW\times SF}$ (1)

Where: $P_{PL}$ is the Payload size (bytes) and $P_{HDR}$ Header size (bytes, typically 13).

The spreading factor $SF$ determines the trade-off between data rate and communication range. The relationship is given by:

$Data\ rate = \frac{Bandwidth\ (BW)}{2^{SF}}$ (2)

Figure 2 illustrates the outlines of the LoRaWAN communication flow, from initialization and network joining to secure data transmission and power-saving modes. It highlights key processes like adaptive data rate adjustment and low-power duty cycling, essential for efficient, long-range IoT connectivity. Figure 3 illustrates the data rate vs spreading factor for different bandwidths at (125 kHz, 250 kHz, or 500 kHz).

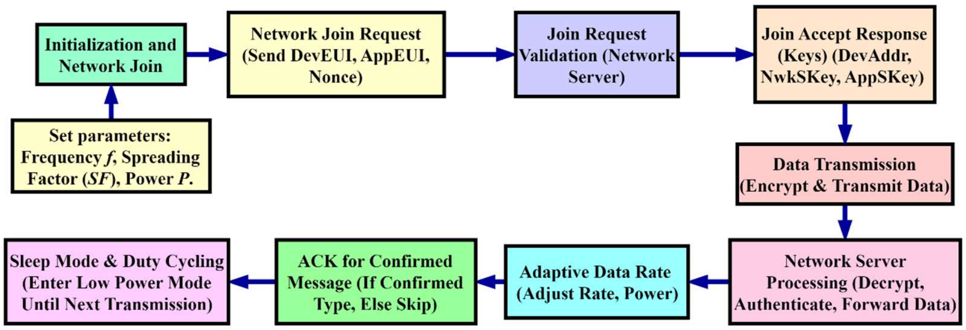


**Figure 2.** LoRaWAN Communication Process Block Diagram**.**

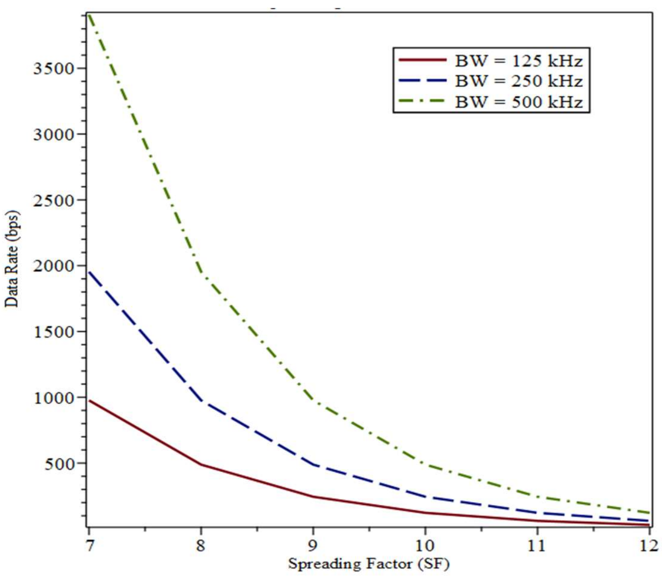


**Figure 3.** Data Rate vs Spreading Factor for Different Bandwidths**.**

2.2.2. SIGFOX Is a Low-Power Wide-Area Network (LPWAN) Protocol

SIGFOX is a low-power wide-area network (LPWAN) protocol designed for simplicity and energy efficiency, utilizing ultra-narrowband (UNB) technology to achieve long-range communication with minimal power consumption. Operating in the unlicensed ISM bands, typically at 868 MHz in Europe and 915 MHz in North America, SIGFOX is particularly suited for applications that require infrequent data transmission. The protocol allows devices to transmit small amounts of data (up to 12 bytes per message) with a maximum of 140 messages per day, ensuring low energy

 doi:10.20944/preprints202603.1394.v1



consumption and extended battery life. The signal-to-noise ratio (SNR) improvement due to UNB can be calculated using the equation[51]:

$$SNR_{Improvement} = 10\log_{10}\left(\frac{BW_{wideband}}{BW_{narrowband}}\right) \quad (3)$$

Where: $BW_{wideband}$ and $BW_{narrowband}$ are the bandwidths of the wideband and narrowband signals, respectively. The narrow bandwidth of SIGFOX (100 Hz) leads to significant SNR improvements, enhancing signal robustness against interference. Additionally, SIGFOX employs Differential Binary Phase-Shift Keying (DBPSK) modulation for uplink communication and Gaussian Frequency-Shift Keying (GFSK) for downlink communication, ensuring efficient and reliable data transmission. The bit error rate (BER) for DBPSK can be approximated using[52]:

$$BER = \frac{1}{2}e^{-\gamma} \quad (4)$$

where $\gamma$ is the signal-to-noise ratio per bit. These features make SIGFOX an ideal choice for scenarios requiring long-range communication, low power consumption, and simple deployment, making it well-suited for wireless sensor networks in applications like environmental monitoring and smart metering. Figure 4 illustrates the SIGFOX communication process, detailing each stage from device initialization to data transmission and cloud processing. The process begins with device initialization, followed by data acquisition, encoding, and compression to fit SIGFOX payload limits. The signal is modulated using Ultra Narrow Band (UNB) technology for efficient long-range transmission and sent to the nearest base station. After base station reception, data is processed on the SIGFOX cloud, forwarded to customer applications, and the device enters sleep mode to conserve power. This streamlined process supports efficient, low-power IoT communications suitable for small data applications.

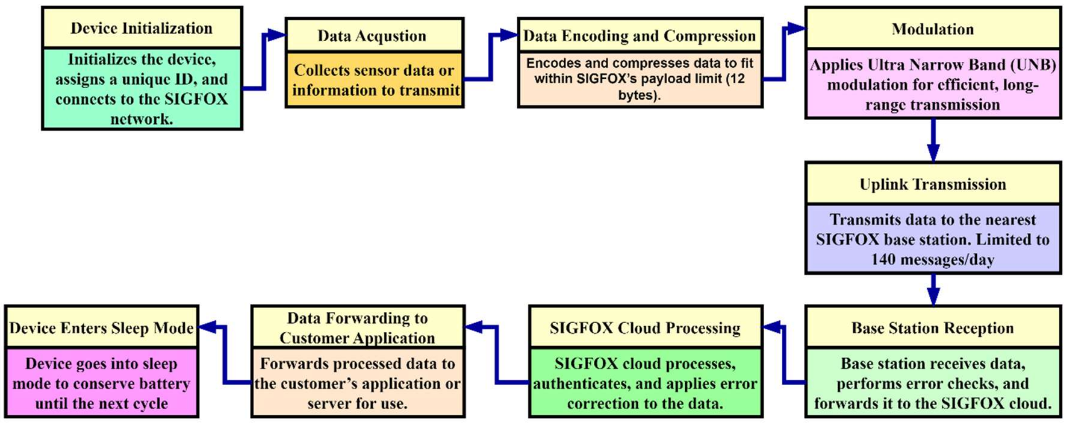


**Figure 4.** SIGFOX Communication Process Block Diagram.

The graph illustrates in **Figure 5** the Bit Error Rate (BER) performance of three modulation schemes DBPSK, BPSK, and QPSK across varying SNR. As expected, BER decreases exponentially with increasing SNR for all schemes, highlighting the improved reliability of communication at higher SNR values. DBPSK demonstrates the highest BER due to its susceptibility to noise, while BPSK achieves better performance owing to its coherent detection. QPSK outperforms both, maintaining the lowest BER across all SNR values due to its higher spectral efficiency and advanced processing. These results emphasize the trade-off between modulation complexity and communication reliability, with QPSK being ideal for scenarios demanding low BER and high data rates, and DBPSK suitable for low-power, low-complexity applications like SIGFOX.

 doi:10.20944/preprints202603.1394.v1



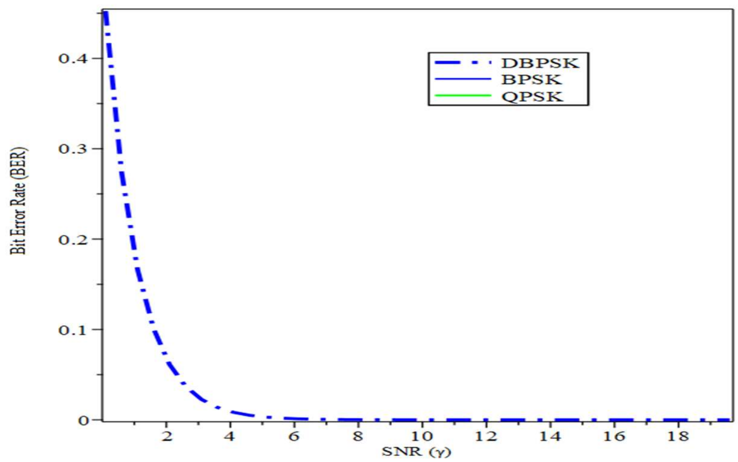


**Figure 5.** Comparison of BER vs SNR for Different Modulation Scheme**.**

2.2.3. Variable Bandwidth Internet of Things (VBIOT)

The VBIOT describes a scheme in which the IoT system will dynamically adjust the device bandwidth allocations with respect to real network conditions and device requirements. Other than classic IoT networks, bandwidth may be fixed or statically allocated. VBIOT introduces flexibility in allowing bandwidth to vary within such parameters as Data Demand, Signal Quality-e.g., Signal-to-Noise Ratio or SNR- and residual energy of every device. The VBIOT system uses different mathematical expressions that determine bandwidth allocation, power control, and energy efficiency[53,54]. These would be designed for optimal performance to prolong the life of the IoT network, dynamically adjusting bandwidth and transmission power based on the real conditions of the network. Below is a mathematical description of the key components in VBIOT.

- Data Demand and Signal-to-Noise Ratio: $D_i$ represent the data demand for device $\boldsymbol{i}$ and $SNR_i$ the signal-to-noise ratio for device $\boldsymbol{i}$. These values are used as inputs to determine bandwidth allocation and power adjustments.
- Bandwidth Allocation: The bandwidth $B_i$ allocated to each device $\boldsymbol{i}$ is a function of its data demand $D_i$, $SNR$, and $SNR_i$ and residual energy $E_{res,i}$. A possible allocation function can be represented as[53,54]:

$B_i = f(D_i, SNR_i, E_{res,i})$. (5)

where $\boldsymbol{f}$ is a function that assigns higher bandwidth to devices with higher data demand and lower $SNR$, while taking into account the available energy.

- Power Control: The transmission power $P_{tx,i}$ for each device is adjusted based on its location and required bandwidth. This can be expressed as:

$P_{tx,i} = g(distance_i, B_i)$. (6)

where $\boldsymbol{g}$ is a function that increases transmission power for devices farther from the receiver to ensure data reliability, while balancing the overall energy consumption.

- Energy Efficiency Calculation: The energy efficiency $\eta_i$ of each device $i$ is calculated to evaluate the network's performance. Energy efficiency is often defined as the ratio of data transmitted per unit of energy consumed:

$\eta_i = \frac{D_i}{E_{consumed,i}}$. (7)

where $E_{consumed,i}$ is the energy used by device iii during transmission. The goal is to maximize $\eta_i$for each device by adjusting $B_i$and $P_{tx,i}$ in real-time.

- Throughput Calculation: The total throughput $\boldsymbol{T}$ of the system, representing the cumulative data transmitted by all devices in the network, is given by:

$T = \sum_i^N B_i$ (8)

where $\boldsymbol{N}$ is the number of devices in the network. Maximizing $T$ while minimizing energy consumption is a key objective of the VBIOT system.

Preprints.org (www.preprints.org) | NOT PEER-REVIEWED | Posted: 18 March 2026 doi:10.20944/preprints202603.1394.v1



- Energy Level Monitoring: Each device's residual energy $E_{res,i}$ is monitored, and adjustments are made to bandwidth and power if $E_{res,i}$ drops below a threshold. This ensures that devices with low energy continue to operate efficiently.

The VBIOT algorithm combines these mathematical relationships to dynamically allocate resources, thereby optimizing power consumption and prolonging the operational lifetime of the IoT network. This approach is particularly effective in applications like nuclear facility monitoring, where both power efficiency and data reliability are essential. Figure 6 presents the VBIOT algorithm designed to optimize power consumption in IoT networks through variable bandwidth allocation. The algorithm involves a sequence of steps: initializing parameters and devices, measuring data demand and signal-to-noise ratio (SNR), allocating bandwidth based on these measurements, controlling transmission power, calculating energy efficiency, transmitting data, monitoring energy levels, and determining if the process should loop or terminate. This adaptive approach adjusts bandwidth and power in real-time, enhancing the efficiency and longevity of IoT networks, particularly in critical monitoring environments like nuclear facilities.

1. ***Start***
   *Initialize parameters and devices.*
2. ***Measure Data Demand & SNR***
   *Input $D_i$ and $SNR_i$ for each device.*
3. ***Bandwidth Allocation***
   *Adjust $B_i$ based on $D_i$, $SNR_i$ and $E_{res,i}$*
4. ***Power Control***
   *Update transmission power $P_{tx,i}$ based on device location.*
5. ***Calculate Efficiency***
   *Compute energy efficiency $\eta_i$ and adjust as needed.*
6. ***Transmit Data***
   *Calculate and update throughput $T$.*
7. ***Monitor Energy Levels***
   *Adjust bandwidth and power if $E_{res,i}$ is low.*
8. ***Repeat or End***
   *Loop or stop depending on the session.*

**Figure 6.** Variable Bandwidth Internet of Things (VBIOT) Algorithm for Power Optimization**.**

### *2.3. Data Aggregation and Compression*

In IoT-based WSNs, data aggregation and compression are essential techniques to optimize energy consumption, reduce data transmission costs, and improve network efficiency. These processes are particularly critical in applications like nuclear facility monitoring, where multiple sensors continuously collect large volumes of data over extended periods[51]. Data aggregation involves collecting and combining data from multiple sensors within a network to eliminate redundancy and reduce the amount of data that needs to be transmitted. Instead of each sensor transmitting its raw data individually, the data is aggregated at an intermediate node or aggregator. This aggregated data, which represents a summarized version of the raw data, is then transmitted to the central base station or server. Mathematically, if multiple sensors in a region produce data values $D_1, D_2, \dots, D_n$ , then an aggregation function $A$ can be applied to generate a representative value $D_{agg}$ such as [51]:

$$D_{agg} = A(D_1, D_2, \dots, D_n) \quad (9)$$

Common aggregation functions include averaging, summation, minimum, and maximum. Data compression further reduces the amount of data by encoding it in a more compact form before transmission. Compression can be either lossless, where the original data can be fully reconstructed, or lossy, where some data accuracy is sacrificed for higher compression ratios. In WSNs, lossless compression is often preferred to maintain data integrity, especially in critical monitoring applications[55].

 doi:10.20944/preprints202603.1394.v1



Compression can be represented as a function $C$, where raw data $D_{agg}$ is transformed into a compressed form $D_{comp}$:

$$D_{comp} = C * D_{agg} \quad (10)$$

Techniques such as Run-Length Encoding ($RLE$), Huffman Coding, and Differential Encoding are commonly used. Advanced methods, such as wavelet-based compression and machine learning-based prediction models, can be applied for higher compression efficiency in complex data environments like nuclear monitoring. Combining aggregation and compression effectively minimizes the data volume that needs to be transmitted, reducing energy consumption significantly. By lowering transmission costs, the network's lifetime is extended, as transmitting data generally consumes more energy than processing it locally. Various data compression algorithms are employed to further reduce the packet size. Compression algorithms like Huffman coding and wavelet-based compression are utilized to decrease the data size without significant loss of information[56]. The effectiveness of these algorithms is evaluated based on their ability to maintain data integrity while reducing transmission overhead.

### *2.4. Battery Management*

Battery health monitoring and smart charging techniques are implemented to extend the operational lifetime of the sensor nodes. Key parameters such as voltage, current, temperature, and impedance are monitored to optimize battery usage [57,58]. Continuous monitoring of battery health parameters helps in identifying and mitigating issues that could affect the battery's performance. This includes tracking voltage, current, temperature, and impedance. Pulse charging is employed as a smart charging technique. It involves charging the battery in short bursts followed by rest periods, which has been shown to improve battery health and longevity. The implementation of pulse charging in the WSN helps in optimizing battery usage and extending the network's operational life.

### *2.5. Routing Protocols for Path Optimization and Data Aggregation*

Several routing protocols are applied to optimize the communication paths among sensor nodes, reducing energy consumption and improving network performance. The protocols evaluated include LEACH, PEBAIS, GAF, and TEEN. Each protocol's performance is assessed based on metrics such as energy consumption, latency, and scalability [43]. The comparative analysis provides insights into the strengths and weaknesses of each protocol, helping to identify the most suitable approach for optimizing power consumption in WSNs for radioactive environment monitoring. Data aggregation is a critical strategy in WSNs aimed at reducing energy consumption and extending network lifetime by eliminating redundant data. This phase leverages a congestion-controlled, data-driven approach to achieve efficient aggregation both locally and globally.

- Local-Level Aggregation: At the node level, redundant data within intra-cluster communication is removed, optimizing the data flow within individual clusters.
- Global-Level Aggregation: At the cluster head (CH) level, redundancy in inter-cluster communication is eliminated to streamline network-wide data transmission.

The data-driven approach adopted in this phase enables in-network processing by utilizing the storage and processing capabilities of sensor nodes, which conserves their energy [6]. This lightweight and energy-efficient method focuses on in-node data aggregation, where cluster members forward data values to the CH via the shortest path. However, congestion may arise due to high traffic. To address this, data is transmitted to the CH through multipath routes using relay nodes, effectively reducing congestion and collision rates. The inclusion of relay nodes significantly enhances the network's lifetime. In this approach, stratified random sampling is employed to create multiple classes, or strata, within each node's buffer. These strata are dynamically designed based on historical data collected by sensor nodes [11]. For instance, in an agricultural irrigation control system, sensor parameters such as soil moisture, temperature, humidity, and wind speed are stored in strata, which adjust dynamically according to seasonal variations and environmental conditions.

The number of strata varies depending on changes in real-time sensed values and environmental conditions within the sensing field. When a cluster member detects a new parameter value, it is stored in the appropriate stratum, ensuring efficient and organized data aggregation across the network. This method enhances both the adaptability and energy efficiency of the WSN.

#### 2.5.1. Low-Energy Adaptive Clustering Hierarchy (LEACH)

The **LEACH** protocol is designed to reduce energy consumption in wireless sensor networks (WSNs) and extend the network's lifetime. The protocol achieves this by dynamically selecting cluster heads (CHs) and rotating their roles among nodes to balance energy usage. The operation of LEACH consists of two phases: the **setup phase** and the **steady-state phase** [7]. In the setup phase, nodes determine whether they will act as CHs based on a probabilistic threshold $T(n)$, which is given by:

$$T(n) = \begin{cases} \frac{p}{1-p(r\ mod(\frac{1}{p})}, n \in G \\ 0, others \end{cases} \quad (11)$$

Where $p$ is the desired percentage of CHs in the network. $r$ is the current round number, and $G$ is the set of nodes that have not been CHs in the last $1/p$ rounds. Nodes that satisfy the threshold broadcast their status as CHs. Non-cluster-head nodes then join the nearest CH based on the received signal strength. During this phase, nodes within a cluster transmit their data to the CH within a **TDMA time slot** [7]. The CH aggregates the data and transmits it to the base station (BS). The energy consumed during data transmission is modeled by the following equations:

$$E_{tx}(k,\gamma) = \begin{cases} k.E_{elec} + k.\varepsilon_{fs}.\gamma^2, \gamma < \gamma_0 \\ k.E_{elec} + k.\varepsilon_{amp}.\gamma^4, \gamma \geq \gamma_0. \end{cases} \quad (12)$$

Where $E_{tx}(k,\gamma)$ is the energy required to send $k$-bit data over a distance $\gamma$. $E_{elec}$ is the Energy consumed per bit for transmission circuitry. $\varepsilon_{fs}$ is the Amplification energy for free-space model. $\varepsilon_{amp}$ is the Amplification energy for multipath fading model. And $d_0$ is the Threshold distance separating free-space and multipath models. The Reception Energy is described as:

$$k_{rx}(k) = k.E_{elec} \quad (13)$$

Where $k_{rx}(k)$ is the energy consumed for receiving $k$-bit data. The Limitations of LEACH: is described as CHs are chosen randomly without considering their residual energy, which can lead to inefficient energy usage if CHs are concentrated in one area or if low-energy nodes are selected as CHs. Direct communication between CHs and the BS can drain the energy of CHs that are farther from the BS. and Frequent re-clustering increases energy consumption, reducing overall network efficiency. Therefore, several improvements over LEACH, such as LEACH-C, PEGASIS, and TPC, address these issues are LEACH-C involves centralized cluster formation by the BS, considering nodes energy levels and locations for CH selection, improving cluster distribution and CH longevity. PEGASIS constructs a chain-based topology for data aggregation, reducing the number of transmissions but requiring periodic chain reconstruction [21]. Energy-Efficient Multi-hop Routing modifies LEACH by introducing multi-hop communication within clusters to save energy.

The threshold $T(n)$ is updated to include the energy factor:

$$T(n) = \frac{p}{1-p(r\ mod(\frac{1}{p})} \cdot \frac{E_i}{E_{average}}, n \in G \quad (14)$$

Where $E_i$ is the residual energy of node iii, and $E_{average}$ is the average energy of all nodes. Figure 7 outlines the key steps of the LEACH Protocol Algorithm. It includes initialization of parameters, cluster head selection, cluster formation, energy consumption during data transmission, metrics calculation, dead node checks, and results storage. The algorithm ensures efficient energy usage and prolongs network lifetime in wireless sensor networks. Figure 8 shows the energy consumption pattern over distance during data transmission. The plotted curve is nonlinear, as energy is consumed quadratically with respect to the amount of transmission distance, which reflects in the steep uphill bend of the graph. For smaller distances, say less than 50 meters, the energy consumed is usually very minimal, which shows the efficiency of data transmission in near-distance communications. However, when the transmission range exceeds 100 meters, its energy consumption rises steeply owing to its relation to distance, especially in the multipath model for long-range distance. This agrees with the first-order radio model, in which energy consumption depends on the square of the distance in free space or on the fourth power in a multipath environment. The results bring into focus the need for an optimal transmission distance to save energy in order to enhance the overall efficiency of wireless sensor networks.

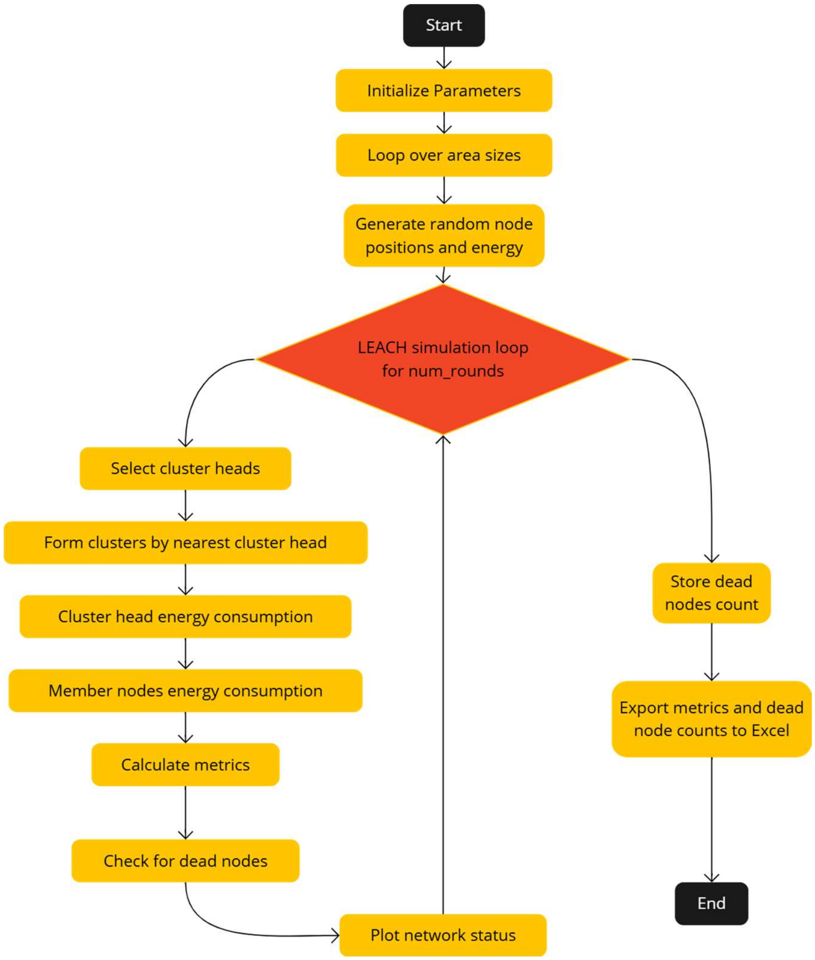


**Figure 7.** Steps of LEACH Protocol Algorithm.

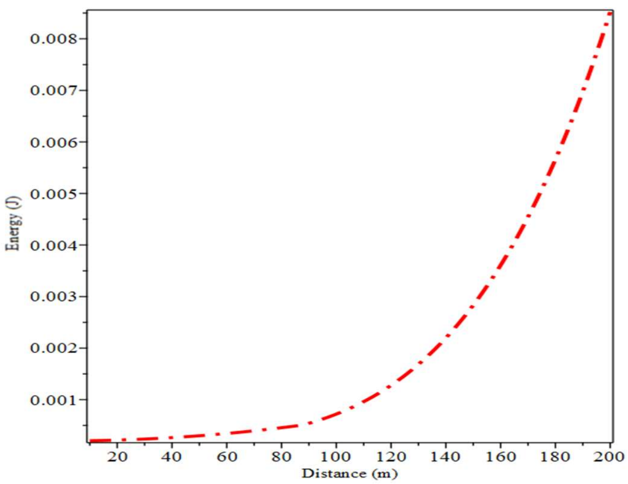


**Figure 8.** Energy Consumption During Transmission.

 doi:10.20944/preprints202603.1394.v1



2.5.2. Power-Efficient and Balanced Aggregation in Sensor Networks (PEBAIS)

The PEBAIS protocol is an energy-efficient data aggregation strategy designed for WSNs. Its primary goal is to extend network lifetime by optimizing energy usage during data transmission while maintaining a balance in power consumption across nodes [59]. The PEBAIS focuses on evenly distributing the energy consumption across all sensor nodes. This ensures that no single node depletes its energy prematurely, which can lead to network partitioning or connectivity issues. Similar to LEACH, PEBAIS employs a hierarchical clustering mechanism. Sensor nodes are grouped into clusters, and each cluster has a designated cluster head (CH) responsible for aggregating and forwarding data. Unlike random CH selection in LEACH, PEBAIS incorporates energy awareness into the CH selection process[43]. Nodes with higher residual energy are more likely to become CHs, which helps to balance the energy load and prevent rapid depletion of energy in critical nodes. To minimize the energy consumed in long-distance transmissions, PEBAIS adopts a multi-hop communication approach. CHs forward aggregated data to the base station (BS) via intermediate CHs, reducing transmission distance and energy costs [7,60]. PEBAIS selects CHs dynamically based on two primary factors: residual energy and distance to the sink. The selection probability for a node iii to become can be represented as:

$$P_{CH}(i) = \alpha \frac{E_i}{E_{max}} + \beta \frac{1}{d_i^2} \quad (15)$$

Where: $E_i$ is the Residual energy of node $i$, $E_{max}$ is the maximum residual energy of any node in the network, $d_i$ Distance of node $i$ to the sink. $\alpha, \beta$ are Weight factors that balance the influence of residual energy and distance. The Energy consumption for a node during data transmission $E_{tx}$ is defined using the first-order radio model:

$$E_{tx}(l,\gamma) = \begin{cases} l.E_e + l.\varepsilon_{fc}.\gamma^2, if\ \gamma < \gamma_0 \\ l.E_e + l.\varepsilon_{mp}.\gamma^4, if\ \gamma \geq \gamma_0 \end{cases} \quad (16)$$

Where: $l$ is the Number of bits in the transmitted data, $\gamma$ is the Energy consumed per bit for transmission electronics, $\varepsilon_{fc}$ is the free-space energy consumption coefficient, $\varepsilon_{mp}$ is the multipath energy consumption coefficient, and $d_0$ is the threshold distance to switch between free-space and multipath models. To reduce redundant data transmissions, PEBAIS employs data aggregation at CHs. The energy cost for aggregating $l$ bits of data at a CH is given by [61]:

$$E_{agg} = l.E_a \quad (17)$$

Where $E_a$ Energy consumed per bit for data aggregation, and the total energy consumption for a CH that aggregates and forwards data from $n$ member nodes is:

$$E_{CH} = \sum_{i=1}^{n}(l_i.E_e + l_i.E_a + l_i.\varepsilon_{fc}.\gamma_i^2) \quad (18)$$

The lifetime of the network, $T_{netwok}$, is defined as the time until the first node dies, which depends on the energy consumption rate [61]:

$$T_{network} = \frac{E_{initial}}{\bar{E}_{cons}} \quad (19)$$

Where $E_{initial}$ is the initial energy of the node, $\bar{E}_{cons}$ is the average energy consumed per node per round.

2.5.3. Power-Efficient and Balanced Aggregation in Sensor Networks (PEBAIS):

PEBAIS focuses on balancing energy consumption across nodes by dynamically adjusting clusters based on current energy levels and data traffic.

2.5.4. Geographic Adaptive Fidelity (GAF):

GAF reduces energy consumption by dividing the network into grids and ensuring only one active node per grid. This approach minimizes the number of active nodes while maintaining network coverage.

 doi:10.20944/preprints202603.1394.v1



2.5.5. Threshold-Sensitive Energy Efficient Sensor Network (TEEN):

TEEN uses hard and soft thresholds to minimize data transmissions, ensuring that only significant changes in the sensed environment trigger data transmission.

## 3. Performance Metrics for Energy Efficiency in Wireless Sensor Networks

When evaluating energy efficiency in wireless sensor networks (WSNs), several key performance metrics are used to assess the effectiveness of protocols, algorithms, and configurations. These metrics provide insights into various aspects of network performance: Energy Consumption per Packet (ECP) quantifies the energy required to transmit a single packet from a source node to a destination node. It helps evaluate the efficiency of data transmission in terms of energy utilization.

$$ECP = \frac{energy\ consumed\ to\ transmit\ a\ packet}{number\ of\ successfully\ transmited\ a\ packets} \quad (18)$$

While Energy Efficiency (EE): EE measures the ratio of data transmitted successfully to the total energy consumed. It provides a comprehensive view of the network energy utilization for data transfer.

$$ECP = \frac{Total\ data\ transmitted\ successfully}{Total\ energy\ consumed} \quad (19)$$

Packet Delivery Ratio (PDR) calculates the ratio of successfully received packets to the total packets sent, reflecting the network's reliability in delivering data.

$$PDR = \frac{Number\ of\ received\ packets}{Number\ of\ sent\ packets} * 100 \quad (20)$$

This metric represents the time until the first node in the network exhausts its energy resources. A longer network lifetime indicates better energy sustainability and efficiency. Network Lifetime=Minimum energy of all nodesEnergy consumption rate of the most

$$Network\ Lifetime = \frac{Minimum\ energy\ of\ all\ nodes}{Energy\ consumption\ rate\ of\ the\ most\ energy\ consuming\ node} \quad (21)$$

Throughput measures the amount of data successfully delivered across the network in a given time frame. While not directly related to energy efficiency, it provides insights into the network's capacity to handle data.

$$Throughput = \frac{Total\ amount\ of\ data\ received}{Total\ Time\ taken\ to\ receive\ the\ data} \quad (22)$$

Sensitivity (Recall or True Positive Rate): Sensitivity is the proportion of true positives (correctly identified events or packets) out of the total actual positives. It evaluates the network's ability to correctly identify and handle critical data.

$$Sensitivity = \frac{True\ Positive}{Total\ Actual\ positive} \quad (23)$$

These metrics collectively provide a detailed assessment of energy efficiency, reliability, and overall performance in WSNs, aiding in the evaluation and optimization of proposed techniques.

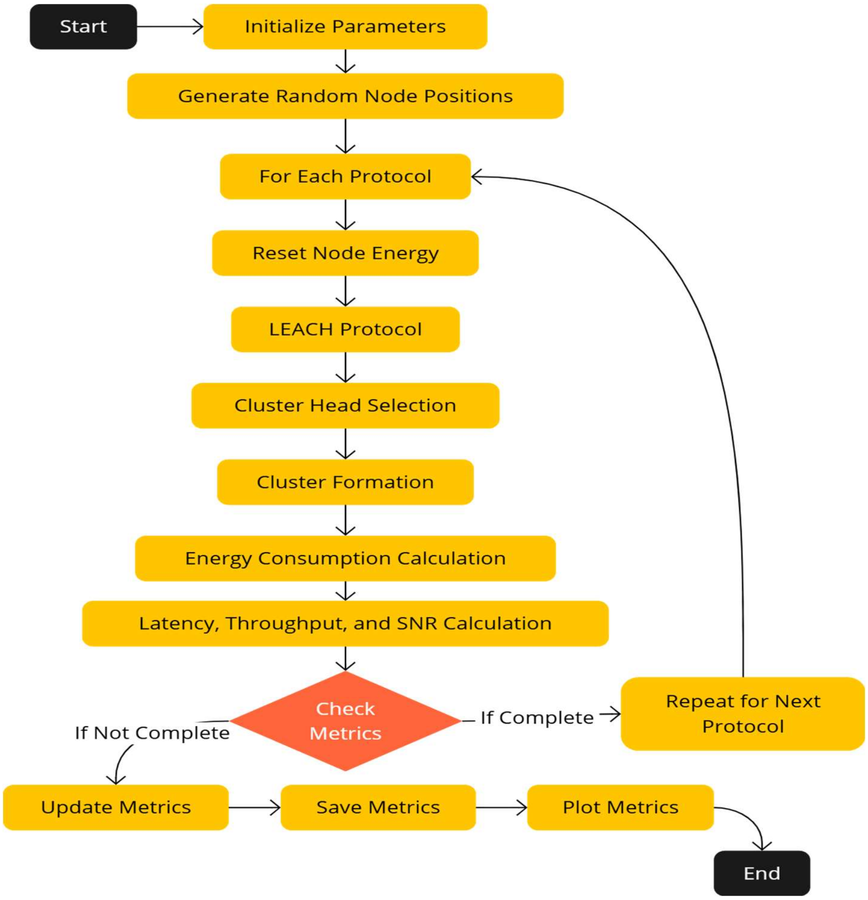


**Figure 9.** Energy Consumption Calculations for different Protocols**.**

## Results and Discussion

The initial phase of the study involved generating synthetic sensor signals to simulate the monitoring of radioactive environments. The sensor signals, represented as sinusoidal waves with added noise, were converted from analogue to digital format using a threshold-based approach. The digital conversion effectively transformed the continuous analogue signals into discrete binary signals, simplifying data processing and transmission. The digital signals retained the essential characteristics of the analogue signals, allowing for efficient monitoring while reducing data size and conserving energy. The study evaluated the performance of three LPWAN protocols - LoRaWAN, SIGFOX, and VBIOT- based on key metrics such as energy consumption, latency, throughput, bit error rate (BER), and signal-to-noise ratio (SNR). Table 1 presents the key parameters used in the study to simulate the performance of a wireless sensor network (WSN). It includes essential details such as the number of sensors, sampling rate, duration of the simulation, and the threshold for binary conversion. Additionally, the table specifies the communication protocol, adaptive data rate setting, transmission power, duty cycle, energy consumption per bit, and battery capacity. These parameters provide a comprehensive overview of the simulation setup, ensuring reproducibility and clarity for readers interested in understanding the experimental conditions and network configuration.

**Table 1.** Simulation Parameters for Wireless Sensor Network.

| Parameter | Value | Unit | Description |
|---|---|---|---|
| Number of Sensors | 50 | - | Total number of sensors in the network |
| Sampling Rate | 100 | Hz | Rate at which sensor data is sampled |
| Duration | 10 | seconds | Total duration of the simulation |

Preprints.org (www.preprints.org) | NOT PEER-REVIEWED | Posted: 18 March 2026 doi:10.20944/preprints202603.1394.v1



| | | | |
|---|---|---|---|
| Time Interval | 0:1/100:10 | - | Time vector for the simulation |
| Threshold | 0 | - | Threshold value for binary signal conversion |
| Duty Cycle (SIGFOX) | 0.01 | - | Duty cycle of the sensors (1%) for SIGFOX |
| Duty Cycle (LoRaWAN) | 0.1 | - | Duty cycle of the sensors (10%) for LoRaWAN |
| Duty Cycle (VBIOT) | 0.05 | - | Duty cycle of the sensors (5%) for VBIOT |
| Energy per Bit (SIGFOX) | $20 \times 10^{-9}$ | Joules | Energy consumption per bit transmitted for SIGFOX |
| Energy per Bit (LoRaWAN) | $50 \times 10^{-9}$ | Joules | Energy consumption per bit transmitted for LoRaWAN |
| Energy per Bit (VBIOT) | $30 \times 10^{-9}$ | Joules | Energy consumption per bit transmitted for VBIOT |
| Battery Capacity | 3600 | Joules | Total battery capacity (equivalent to 1 Wh) |

### *4.1. Energy Consumption Comparison*

Figures 10 through 14 provide a detailed comparative analysis of the performance metrics for 50 sensors using SIGFOX, LoRaWAN, and VBIOT protocols. Figure 10 illustrates the energy consumption across the three protocols, measured in Joules, with SIGFOX ranging from approximately $9.8 \times 10^{-6}$ Joules to $1.1 \times 10^{-5}$ Joules, LoRaWAN ranging from $2.45 \times 10^{-5}$ Joules to $2.7 \times 10^{-5}$ Joules, and VBIOT ranging from $7.5 \times 10^{-6}$ Joules to $8.2 \times 10^{-6}$ Joules. These variations highlight differences in sensor activities and communication efficiencies among the protocols. Figure 11 shows the latency for data transmission, with all protocols fluctuating between 5.1 and 5.4 seconds, indicating the time required for data to travel from sensors to the network server. Figure 12 presents the throughput, with values ranging from 50 to 54 bits per second across all protocols, indicating the rate at which data is successfully transmitted over the network. Figure 13 depicts the network lifetime, with SIGFOX ranging from approximately $3.3 \times 10^{7}$ seconds to $3.7 \times 10^{7}$ seconds, LoRaWAN ranging from $1.32 \times 10^{8}$ seconds to $1.46 \times 10^{8}$ seconds, and VBIOT ranging from $4.4 \times 10^{7}$ seconds to $4.8 \times 10^{7}$ seconds. These variations underscore the impact of energy consumption and efficiency on the overall durability of the wireless sensor network. Figure 14 compares the SNR, with values ranging from 16.5 to 20.5 dB, reflecting the quality of the communication signal relative to background noise across the protocols. Collectively, these figures demonstrate the distinct advantages and trade-offs of each protocol in terms of energy efficiency, latency, throughput, network lifetime, and SNR, which are crucial for reliable and sustainable monitoring in radioactive environments.

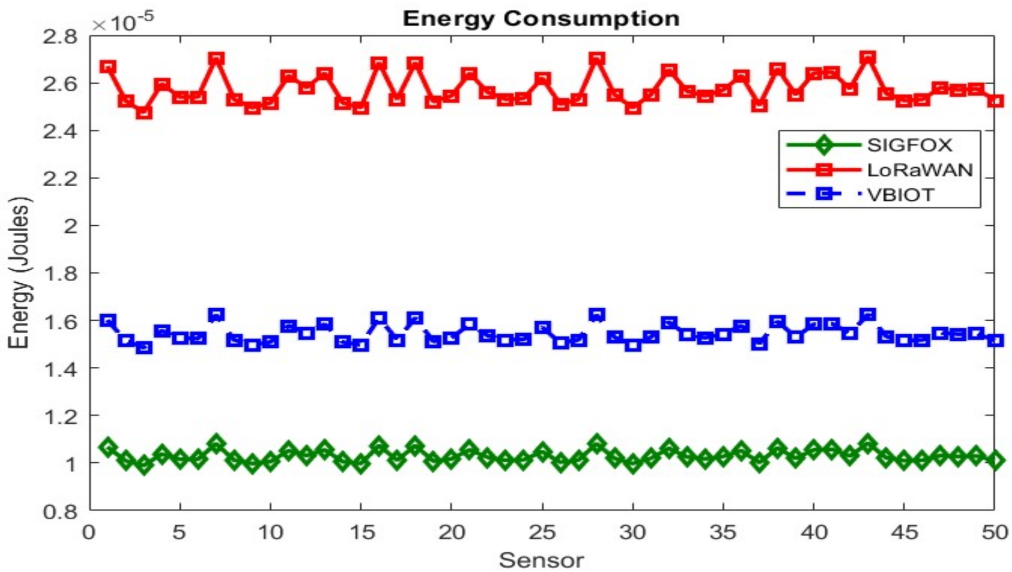


**Figure 10.** Energy Consumption Comparison Across Protocols**.**

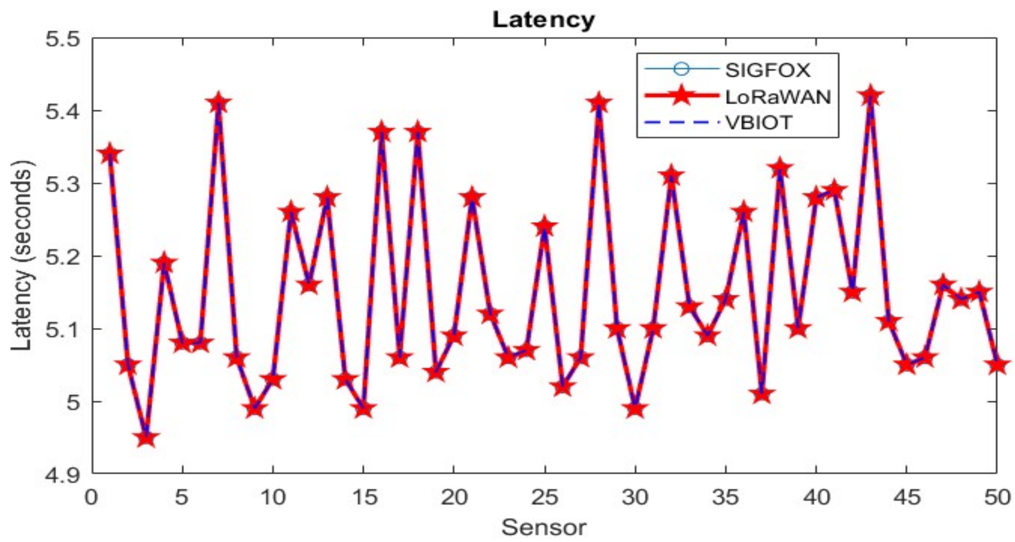


**Figure 11.** Latency Comparison Across Protocols.

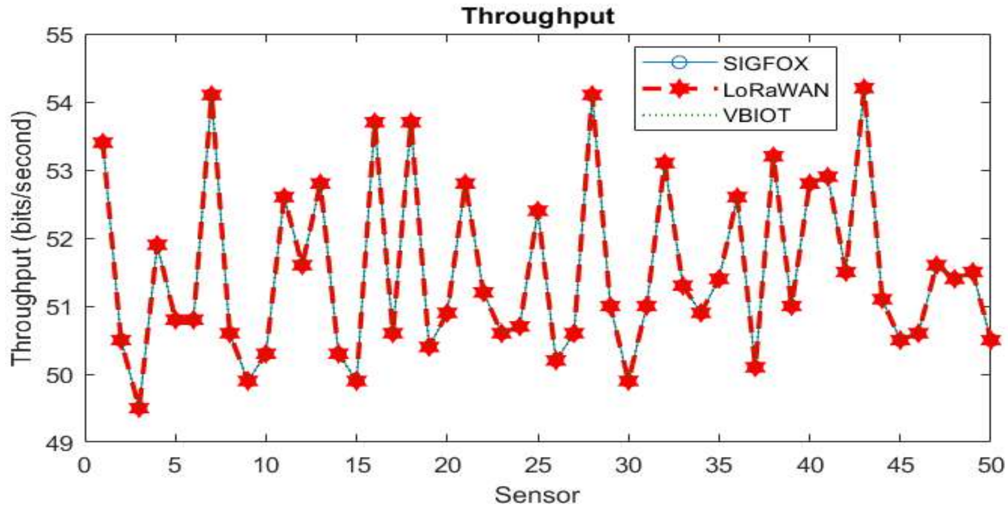


**Figure 12.** Throughput Comparison Across Protocols.

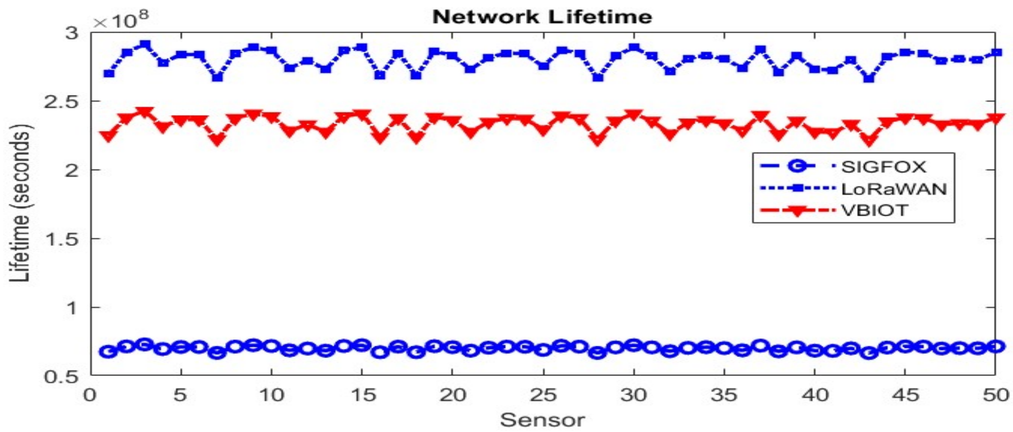


**Figure 13.** Network Lifetime Comparison Across Protocols.

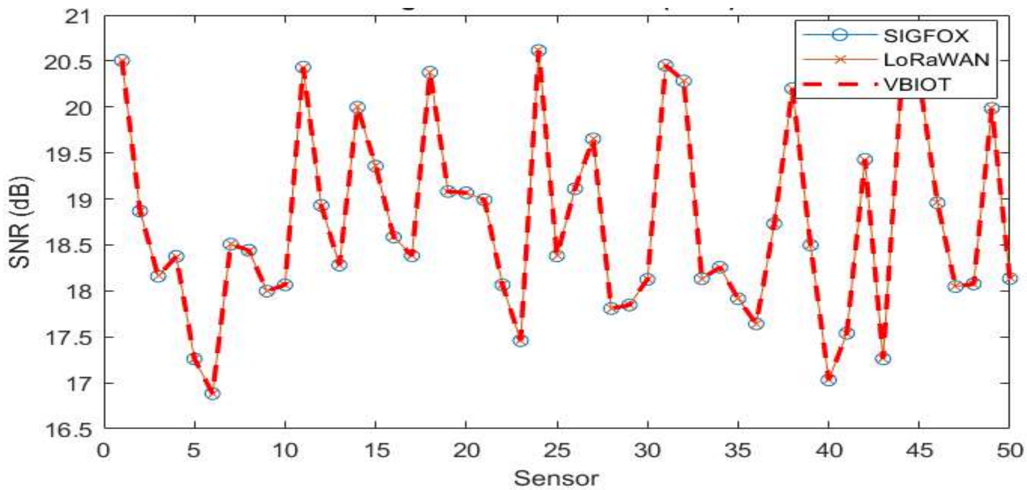


**Figure 14.** Signal-to-Noise Ratio (SNR) Comparison Across Protocols**.**

*4.2. Data Aggregation and Compression*

The data aggregation process integrated readings from multiple sensors, reducing redundancy and conserving energy. Various compression algorithms, such as Huffman coding and wavelet-based compression, were employed to decrease data size without significant loss of information. The effectiveness of these techniques was evident in the reduced transmission overhead and maintained data integrity, highlighting their importance in optimizing power consumption for WSNs. The methodology involved generating synthetic data for a network of 50 sensors, each producing 100 samples. Data aggregation was achieved using K-means clustering, forming 5 clusters and averaging the data within each cluster to reduce noise and volume. The aggregated data was then compressed using Huffman coding, with dictionaries created based on symbol frequencies. Data integrity was verified through decompression. Energy consumption was based on the number of compressed bits and energy per bit; latency on transmission time; throughput on data rate; BER was assumed zero; network lifetime on battery capacity and energy use; and SNR assessed data quality. Additionally, battery health parameters, including voltage (3.7 V), current (0.5 A), temperature (25 °C), and impedance (0.05 Ω), were monitored to ensure optimal performance and longevity. Visualization of these metrics highlighted the performance benefits and trade-offs of the aggregation and compression methods, optimizing sensor network efficiency and longevity. This robust analysis is essential for reliable, sustainable monitoring in complex environments. The results illustrated at Figures 15 through 17 provide a detailed analysis of data aggregation and signal quality metrics for a wireless sensor network. Figure 15 demonstrates the effectiveness of the data aggregation process, with the top panel displaying highly variable and noisy original sensor data, and the bottom panel showing significantly reduced noise and variability in the aggregated data, enhancing its clarity and usability. Figure 16 illustrates the SNR across different clusters, measured in dB, highlighting variations in data quality, with higher SNR values indicating better data integrity. Figure 17 offers a comprehensive comparison of performance metrics, including Energy Consumption, Latency, Throughput, BER, Network Lifetime, and SNR, across different clusters using a radar chart. This visual assessment reveals the strengths and weaknesses of each cluster, aiding in the optimization of the wireless sensor network for specific application requirements. Collectively, these figures underscore the importance of data aggregation in improving sensor data quality and provide insights into optimizing network performance across various metrics. Table 1 provides a comprehensive overview of key sensor metrics, including energy consumption, latency, throughput, bit error rate (BER), network lifetime, and SNR. The energy consumption values range from $2.16 \times 10^{-5}$ Joules to $3.36 \times 10^{-5}$ Joules, reflecting the power required by the sensors for operation. Latency values vary significantly, with some sensors exhibiting a latency of 4.32 seconds while others reach up to 67.2 seconds, indicating differences in data transmission times across the network. Throughput, measured in bits per second, shows high efficiency in most cases, with values around 617.142857 and 672 bits per second, except for a lower throughput value of 67.2 bits per second observed in one instance. The BER remains at zero across all sensors, signifying error-free data transmission. Network lifetime, which is crucial for long-term monitoring applications, varies from 29761.90476 seconds to 297619.0476 seconds, influenced by the energy consumption rates. SNR values, ranging from 8.89921988 to 17.2802588 dB, indicate the quality of the signal relative to background noise, with higher values representing better signal clarity. This table underscores the importance of optimizing these metrics to enhance the performance and reliability of wireless sensor networks in monitoring applications.

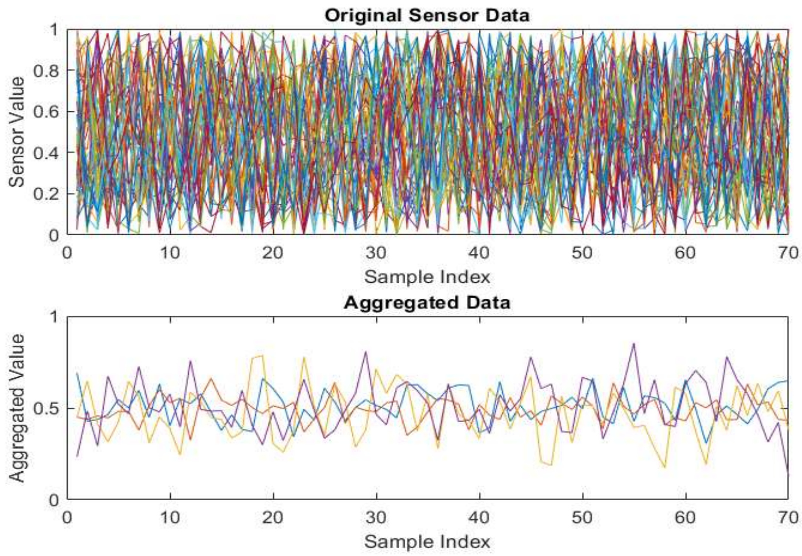


**Figure 15.** Original Sensor Data and Aggregated Data**.**

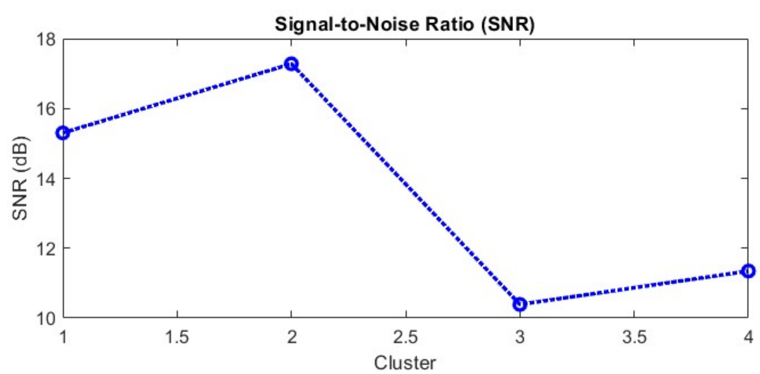


**Figure 16.** Signal-to-Noise Ratio (SNR) Across Clusters**.**

doi:10.20944/preprints202603.1394.v1



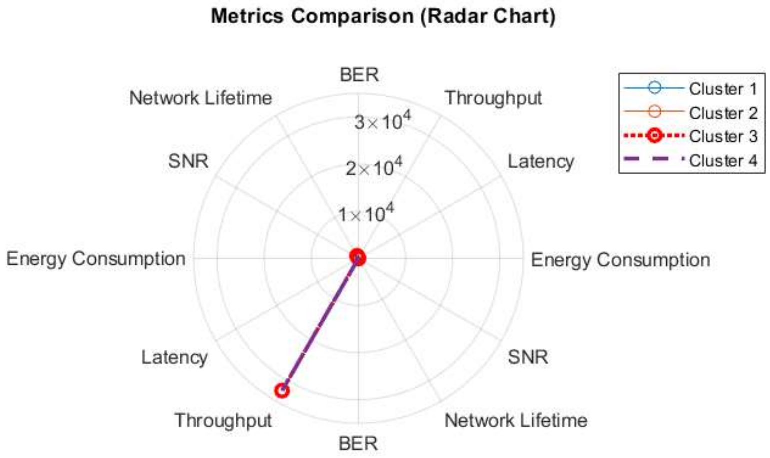


**Figure 17.** Metrics Comparison (Radar Chart)**.**

**Table 2.** A comprehensive overview of key sensor metrics.

| Energy Consumption | Latency | Throughput | BER | Network Lifetime | SNR |
|---|---|---|---|---|---|
| $2.16 \times 10^{-5}$ | 4.32 | 617.142857 | 0 | 32407.40741 | 15.3012018 |
| $2.16 \times 10^{-5}$ | 4.32 | 617.142857 | 0 | 32407.40741 | 17.2802588 |
| $2.16 \times 10^{-5}$ | 4.32 | 617.142857 | 0 | 32407.40741 | 10.3894456 |
| $2.16 \times 10^{-5}$ | 4.32 | 617.142857 | 0 | 32407.40741 | 11.3458571 |
| $3.36 \times 10^{-5}$ | 67.2 | 67.2 | 0 | 297619.0476 | 12.813589 |
| $3.36 \times 10^{-5}$ | 6.72 | 672 | 0 | 29761.90476 | 8.89921988 |
| $3.36 \times 10^{-5}$ | 6.72 | 672 | 0 | 29761.90476 | 9.88349404 |
| $3.36 \times 10^{-5}$ | 6.72 | 672 | 0 | 29761.90476 | 10.8876542 |
| $3.36 \times 10^{-5}$ | 6.72 | 672 | 0 | 29761.90476 | 10.5238555 |
| $3.36 \times 10^{-5}$ | 6.72 | 672 | 0 | 29761.90476 | 12.394339 |

### *4.3. Battery Management*

Battery health monitoring and smart charging techniques significantly extended the operational lifetime of the sensor nodes. Monitoring key parameters like voltage, current, temperature, and impedance allowed for optimal battery usage. Pulse charging, involving short bursts of charging followed by rest periods, improved battery health and longevity. These strategies ensured that the WSN could operate continuously with minimal maintenance, essential for monitoring radioactive environments. Figures 18 and 19 provide a detailed analysis of the pulse charging process and its impact on battery performance. Figure 18a illustrates the cyclical nature of pulse charging, where a current of 1 A is applied for 10-second intervals, followed by 5-second rest periods. This approach aims to enhance battery longevity by allowing recovery periods between charging pulses. Figure 18b shows the corresponding voltage changes during these cycles, with the voltage increasing during the charging phases and slightly decreasing during rest periods, reflecting the dynamic response of the battery to pulse charging.

 doi:10.20944/preprints202603.1394.v1



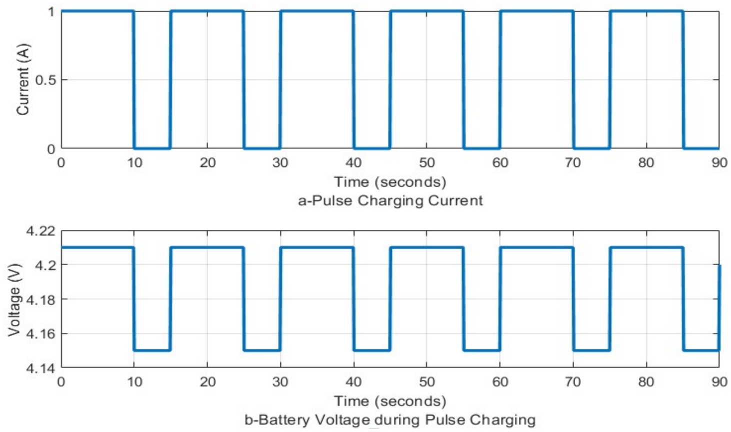


**Figure 18.** a. Pulse Charging Current vs. Time, b. Battery Voltage vs. Time during Pulse Charging**.**

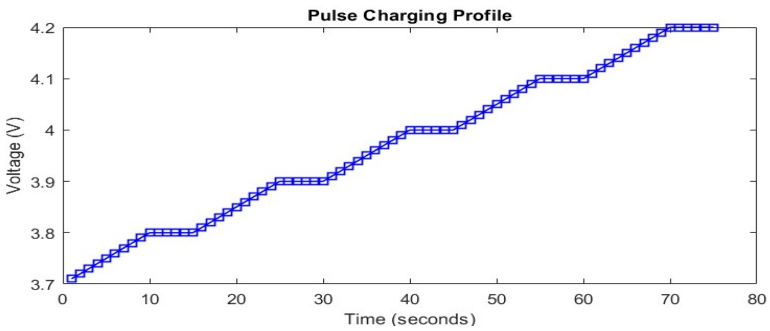


**Figure 19.** Pulse Charging Profile**.**

Figure 19 offers a comprehensive view of the overall voltage profile during the entire pulse charging process. The voltage incrementally rises from 3.7 V to over 4.2 V, demonstrating the cumulative effect of the pulse charging cycles. This stepwise increase underscores the effectiveness of pulse charging in steadily enhancing battery voltage while mitigating the risks of overcharging and thermal buildup, thus promoting battery health and extending its operational life. These figures collectively highlight the advantages of pulse charging as a method to optimize battery performance in wireless sensor networks and other applications requiring reliable and long-lasting power sources. While Figure 20 block diagram of Battery health monitoring using Huffman coding

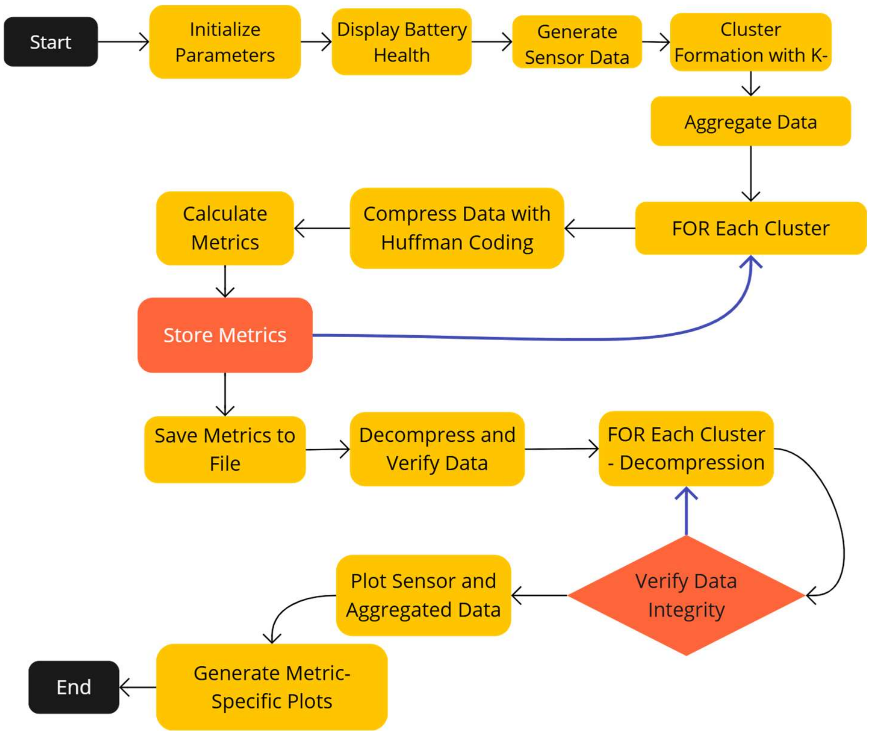


**Figure 20.** block diagram of Battery health monitoring using Huffman coding**.**

*4.4. Routing Protocols for Path Optimization*

The evaluation of routing protocols- LEACH, PEBAIS, GAF, and TEEN- provided insights into their performance in terms of energy efficiency, latency, and scalability.

4.4.1. Geographic Adaptive Fidelity (GAF)

Reduced energy consumption by dividing the network into grids and ensuring only one active node per grid, maintaining network coverage. Figures 21 and 22 provide a comprehensive analysis of the Geographic Adaptive Fidelity (GAF) protocol performance in a wireless sensor network with 100 nodes, each initialized with 0.5 Joules of energy, deployed over a 5000 $m^2$ area. The sink is centrally positioned at coordinates [500, 500], and the simulation spans ten rounds. Figure 21 illustrates the spatial distribution of nodes during the ninth simulation round, distinguishing between active and regular nodes and highlighting communication pathways to the sink. This visualization showcases the GAF protocol effectiveness in maintaining network connectivity and managing node activity within a grid size of 10x10 meters. While Figure 22 presents detailed insights into key performance metrics over ten simulation rounds. Energy consumption remains stable around 58 Joules per round, indicating efficient energy management. Latency is consistently approximately 1 second per round, ensuring timely data transmission. Throughput remains steady at 100 bits per second, reflecting reliable data transfer rates. The BER is consistently zero, demonstrating the protocol robustness in minimizing transmission errors. Network lifetime exhibits variability but generally sustains around five rounds, balancing energy consumption and node activity.

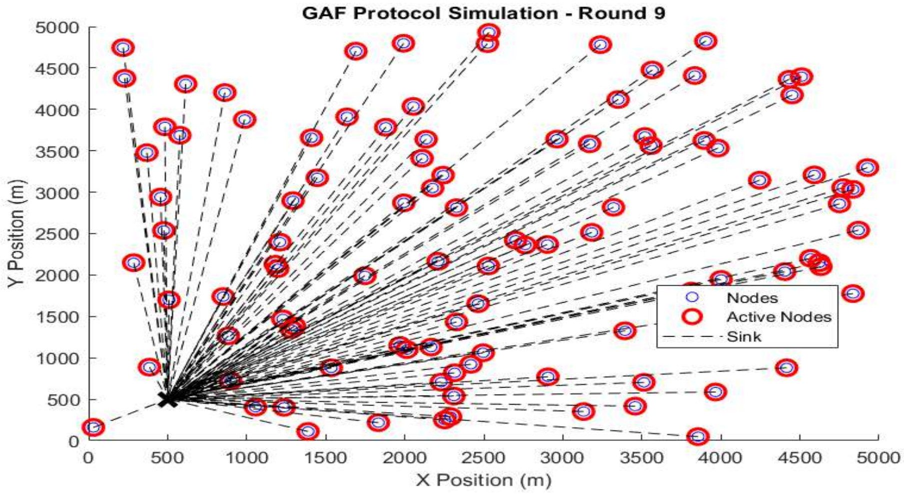


**Figure 21.** GAF Protocol Simulation - Round 9 under the GAF protocol.

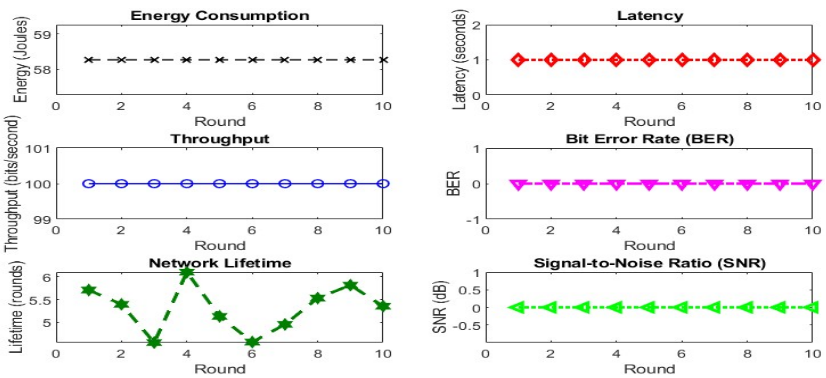


**Figure 22.** Performance Metrics over Rounds under the GAF protocol.

The SNR fluctuates slightly around 0.5 dB, indicating consistent signal quality. Additionally, the node mortality data across the simulation rounds provide critical insights into the network's resilience: Round 1 saw 51 nodes dead, increasing to 69 by Round 2, 76 by Round 3, 86 by Round 4, and stabilizing around 90-93 dead nodes by Rounds 7-10. This progression highlights the GAF protocol ability to extend network longevity and manage node energy efficiently despite the increasing number of inactive nodes.

4.4.2. Low-Energy Adaptive Clustering Hierarchy (LEACH) Protocol

LEACH The protocol minimized path length by organizing nodes into clusters and rotating the cluster head (CH) role, balancing energy consumption among nodes. Figures 23 and 24 provide a detailed analysis of the LEACH protocol performance in a wireless sensor network with 100 nodes, spanning ten simulation rounds. The simulation parameters include a network area of 5000 m$^2$, with nodes initialized with 0.5 Joules of energy each. The sink is centrally positioned at coordinates [500, 500], and each data packet size is set to 4000 bits, with an energy consumption of 50x10$^{-9}$ Joules per bit. Figure 23 illustrates the node positions and cluster formations during the tenth round, with blue circles representing nodes, red circles as cluster heads, and the sink marked by a black cross. The dashed lines show communication paths from nodes to cluster heads and from cluster heads to the sink, depicting the network topology and data aggregation paths. Figure 24 presents key performance metrics over the simulation rounds. Energy consumption shows significant fluctuations, particularly peaking in round 8, highlighting varied energy usage across rounds. Latency, representing the time taken for data transmission, also fluctuates, with a notable increase in round 8, impacting the overall network response time. Throughput remains stable at around 400,000 bits per second, indicating consistent data transfer rates. The Bit Error Rate (BER) stays at zero, demonstrating reliable communication without data corruption. Network lifetime decreases sharply after the first round and stabilizes at a low value, reflecting rapid energy depletion in initial rounds. The SNR fluctuates around 0.001 dB, indicating the quality of the signal relative to background noise, with lower values suggesting challenges in maintaining high-quality signal transmission.

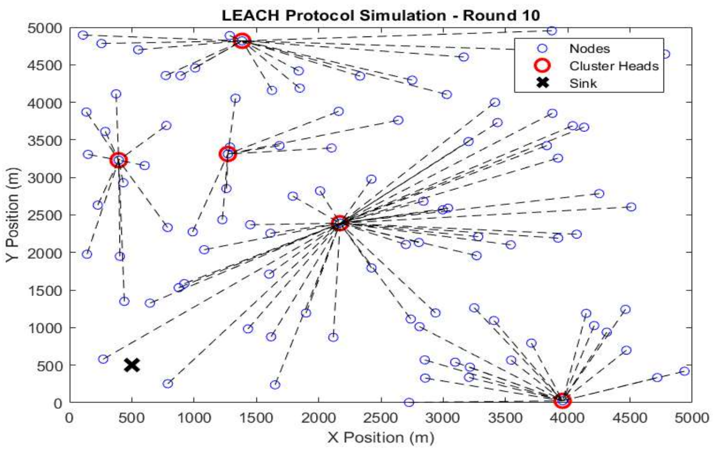


**Figure 23.** The network topology and data aggregation paths under the LEACH protocol**.**

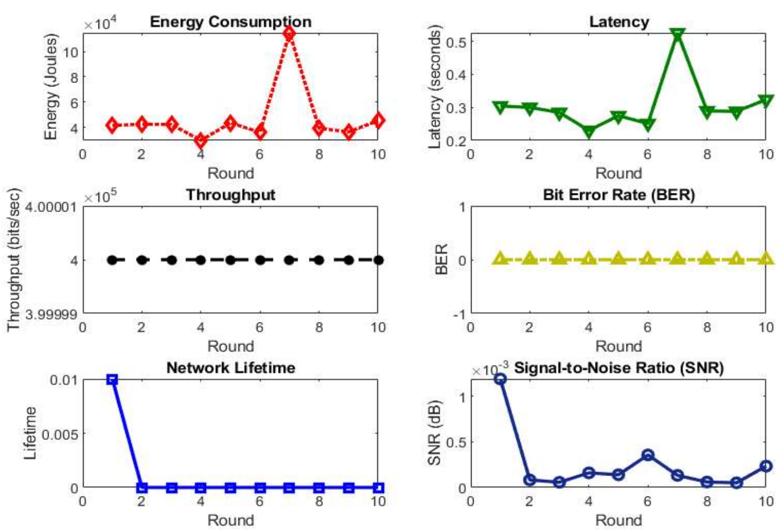


**Figure 24.** Performance metrics of the LEACH protocol over ten simulation rounds**.**

4.4.3. Power-Efficient and Balanced Aggregation in Sensor Networks (PEBAIS)

PEBAIS Focused on balancing energy consumption dynamically, ensuring even distribution of energy usage across the network. Figures 25 and 26 provide an in-depth analysis of the PEBAIS protocol performance in a wireless sensor network with 200 nodes, spanning ten simulation rounds. The simulation parameters include a network area of 5000 m², with nodes initialized with 0.5 Joules of energy each, a centrally positioned sink at coordinates [500, 500], and a data packet size of 4000 bits with an energy consumption of $50x10^{-9}$ Joules per bit. The cluster threshold for cluster head selection is set at 0.1, with a sampling rate of 100 Hz and a duration of 1 second for simplicity. During the simulation, the number of dead nodes increases progressively across the rounds, with 108 nodes dead by round 1, 127 by round 2, 134 by round 3, 146 by round 4, 154 by round 5, 169 by round 6, 172 by round 7, 175 by round 9, and 176 nodes dead by round 10. Figure 25 illustrates the node positions and cluster formations during the tenth round, with blue circles representing nodes, red circles as cluster heads, and the sink marked by a black cross. The dashed lines show communication paths from nodes to cluster heads and from cluster heads to the sink, depicting the network topology and data aggregation paths under the PEBAIS protocol. Figure 26 presents key performance metrics over the simulation rounds. Energy consumption initially drops significantly after the first few rounds, stabilizing thereafter, indicating the protocol's efficiency in managing energy usage. Latency stabilizes around 2 seconds after the initial rounds, reflecting consistent network response times. Throughput increases sharply in the initial rounds and stabilizes at around 200 bits per second, suggesting efficient data transfer capabilities. The BER remains at zero throughout the simulation, demonstrating the protocol's reliability in ensuring error-free communication. Network lifetime exhibits fluctuations, peaking around round 3 and stabilizing subsequently, highlighting the impact of energy-efficient protocols on network durability. The SNR fluctuates between 12 and 16 dB, indicating variations in signal quality relative to background noise, with higher values suggesting better signal quality.

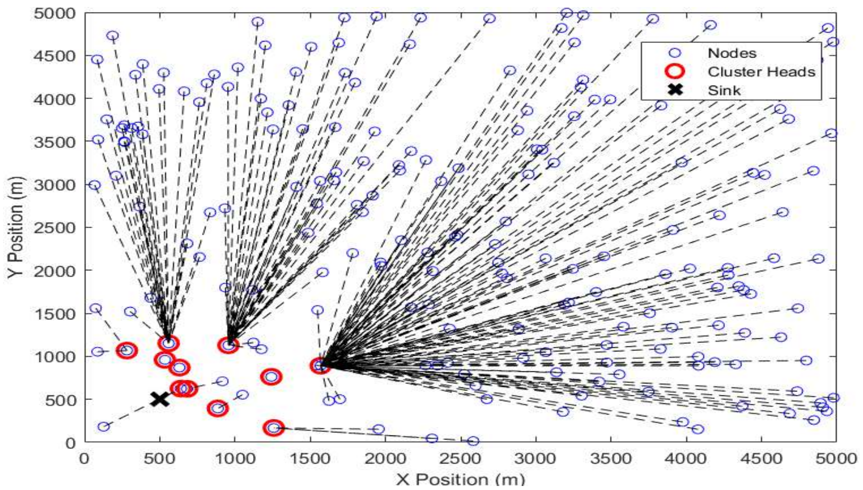


**Figure 25.** Simulation - Round 10 for the network topology and data aggregation paths under the PEBAIS protocol.

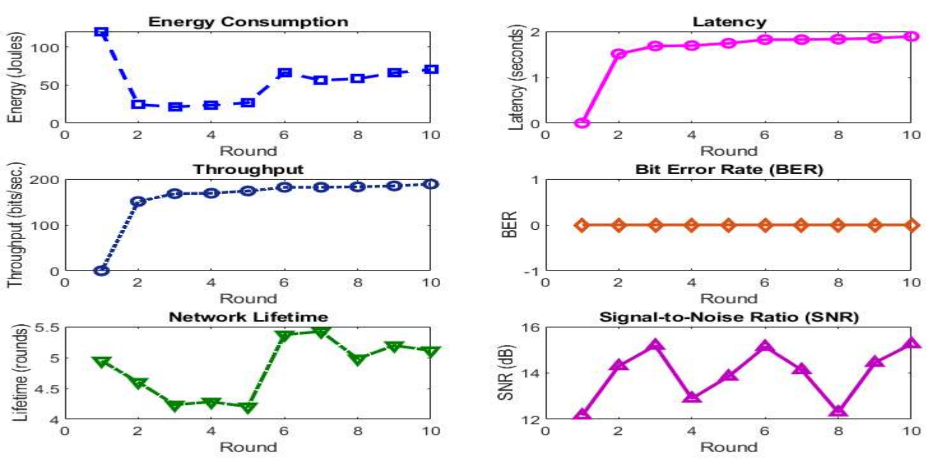


**Figure 26.** Performance metrics of the PEBAIS protocol over ten simulation rounds.

4.4.4. TEEN

Figure 27 illustrates the network configuration for the TEEN (Threshold-sensitive Energy Efficient sensor Network) protocol during round 10, depicting the nodes (blue circles), cluster heads (red circles), and the sink (black cross). Dashed black lines denote the communication pathways among the nodes, cluster heads, and the sink. The illustration emphasizes the effective aggregation of nodes beneath cluster heads, hence diminishing the direct communication burden on the sink. TEEN enhances energy efficiency by prioritizing event-driven data transmission, transmitting only essential data, hence extending network longevity. This configuration illustrates TEEN's efficacy in facilitating energy-efficient transmission, crucial for sustained monitoring in a radioactive setting.

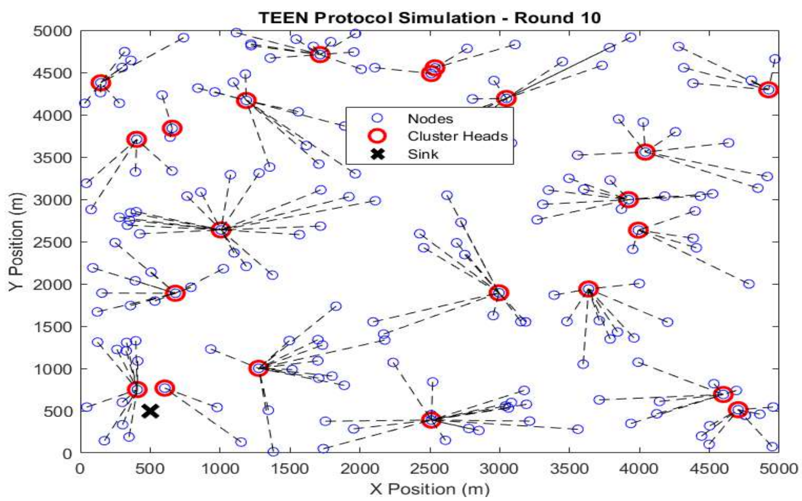


**Figure 27.** TEEN Protocol Simulation - Round 10: Network Topology with Cluster Heads and Sink.

Figure 28 shows six important parameters from the TEEN protocol's performance analysis throughout 30 rounds. Variations in network activity and energy usage are shown by fluctuations in energy consumption, which ranges from 12 to 22 Joules. Consistent network responsiveness is reflected by the stable latency, which fluctuates little between 0.16 and 0.17 seconds. Network congestion or node energy depletion may be the cause of the intermittent changes in throughput, which range from 160 to 175 bits/second. The data transfer is error-free because the bit error rate (BER) remains at zero. An ever-decreasing network lifetime indicates a slow but steady drain on available energy resources. Finally, the signal-to-noise ratio (SNR) remains within an acceptable range of 11.5 to 12 dB, indicating that the signal quality is good in comparison to the noise. While energy depletion does reduce the network's lifetime, the TEEN protocol shows consistent communication performance overall.

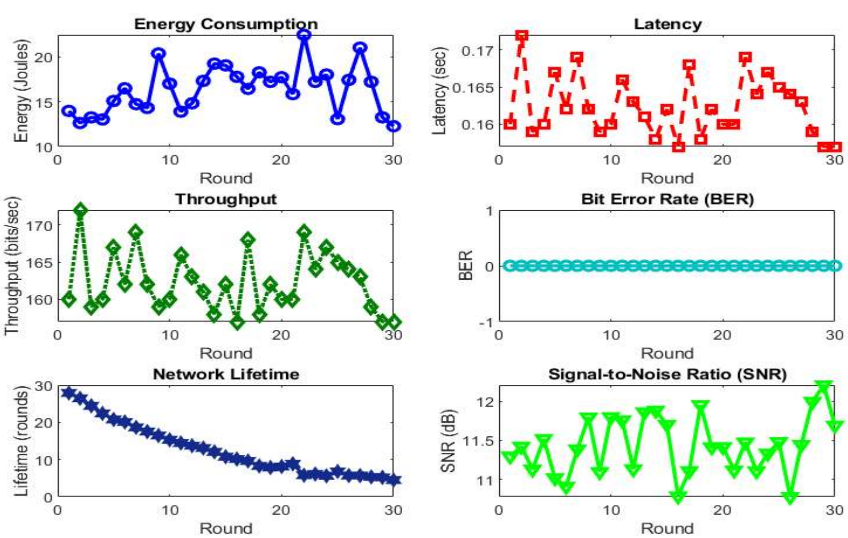


**Figure 28.** Performance metrics of the TEEN protocol over ten simulation rounds.

 doi:10.20944/preprints202603.1394.v1



*4.5. Dead Nodes per Round for Different Area Sizes with Different Protocols*

In this simulation study, we deployed 200 sensor nodes randomly within an area of 5000 square meters. Each node was initialized with an initial energy of 0.5 Joules. The sink node was centrally located at coordinates [500, 500], serving as the data collection point. The simulation ran for 30 rounds, with each round representing a communication cycle between the nodes and the sink. Data packets transmitted by the nodes had a fixed size of 4000 bits, and the energy consumption per bit was set to 50 nanojoules. The sampling rate during data transmission was maintained at 100 Hz, with the overall simulation assuming a unit time duration of 1 second per round. Additionally, specific parameters were tailored for each protocol: LEACH used a cluster head selection probability of 0.1, while PEBAIS and TEEN employed an energy threshold of 0.1 for cluster head selection. For the GAF protocol, the grid size was set to 100 meters for efficient grid formation. Throughout the simulation, the performance of each protocol was assessed in terms of energy consumption, latency, throughput, bit error rate (BER), network lifetime, and signal-to-noise ratio (SNR), with results stored for comparative analysis. Figure 29 illustrates the effect of varying area sizes (1000 to 5000 meters) on the quantity of inactive nodes per round within the PEBAIS protocol. As the area size expands, the quantity of dead nodes grows markedly, indicating the energy strain imposed on nodes in greater regions due to prolonged communication distances. In the smallest area (1000 meters), nodes maintain prolonged activity, exhibiting little fatalities until the latter rounds. Conversely, the larger area sizes (3000, 4000, and 5000 meters) exhibit a swift escalation in node mortality, with nearly all nodes exhausted by round 20 in the 5000-meter area. The findings indicate that larger area sizes exacerbate energy consumption, leading to an increase in node failures and a decrease in network longevity. This analysis highlights the necessity of optimising protocols such as PEBAIS for energy efficiency in extensive networks, especially in applications like environmental or radioactive monitoring, where long-term network sustainability is essential. The simulation in Figure 30 demonstrates the TEEN (Threshold-sensitive Energy Efficient Sensor Network) protocol's efficacy in a range of area sizes, from 1000 to 5000 meters. The number of dead nodes increases gradually as the cycles progress, with larger area sizes resulting in a more rapid depletion of node energy, as illustrated by the graph. For example, by round 20, nearly 180 nodes have perished in the 5000-meter area, whereas only a handful of nodes have expired in the 1000-meter area. This trend is consistent across all area sizes, suggesting that larger areas place a greater strain on node energy, primarily as a result of longer communication distances. Consequently, this leads to increased energy consumption and earlier node mortality. The longevity and efficiency of the network under the TEEN protocol are significantly influenced by the extent of the area, as illustrated in the figure. There are different areas from 1000 meters to 5000 meters shown in Figure 31 that show how the LEACH (Low-Energy Adaptive Clustering Hierarchy) strategy works in terms of the number of dead nodes per round. The results make it clear that the number of dead nodes rises faster as the area gets bigger. By round 20, there are almost 160 dead nodes in the largest area (5000 meters), which means that a lot of energy has been used up. But when the area is smaller, like between 1000 and 2000 meters, the node survival rate is much higher, and there are fewer dead nodes during the exercise. The LEACH system uses less energy in smaller areas because nodes can keep their energy for longer because they can communicate more easily. This picture shows how important area size is for figuring out how much energy is used and how long the network lasts when using the LEACH protocol. Figure 32 depicts the quantity of deceased nodes per round over various area dimensions (spanning from 1000 to 5000 meters) using the GAF (Geographic Adaptive Fidelity) protocol. The picture illustrates a distinct pattern indicating that bigger area sizes, specifically 5000 and 4000 meters, lead to a more accelerated rise in dead nodes, surpassing 180 by round 6 for the largest area. Conversely, lower area sizes, such as 1000 meters, have markedly fewer dead nodes, with nearly no nodes failing even by the 20th round. This pattern indicates that the protocol's energy efficiency is significantly influenced by the area size, with larger regions resulting in increased communication costs and energy consumption for the nodes. The GAF protocol's approach, which conserves energy by placing nodes in a dormant

 doi:10.20944/preprints202603.1394.v1



state while preserving integrity, demonstrates efficacy in smaller regions. In expansive regions, the augmented distances between nodes and the sink swiftly deplete energy supplies, resulting in a significant increase of inactive nodes.

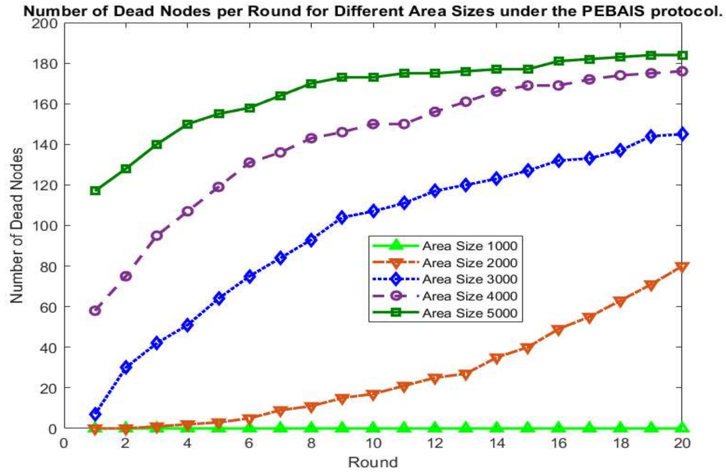


**Figure 29.** Number of Dead Nodes per Round for Different Area Sizes under the PEBAIS Protocol**.**

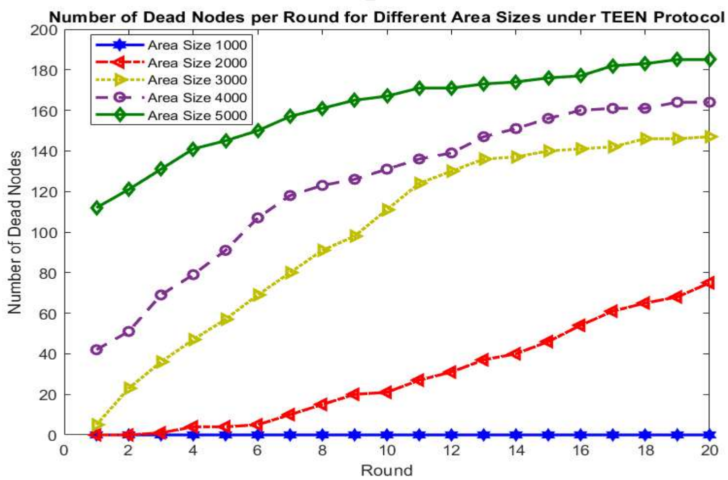


**Figure 30.** Number of Dead Nodes per Round for Different Area Sizes under the TEEN Protocol**.**

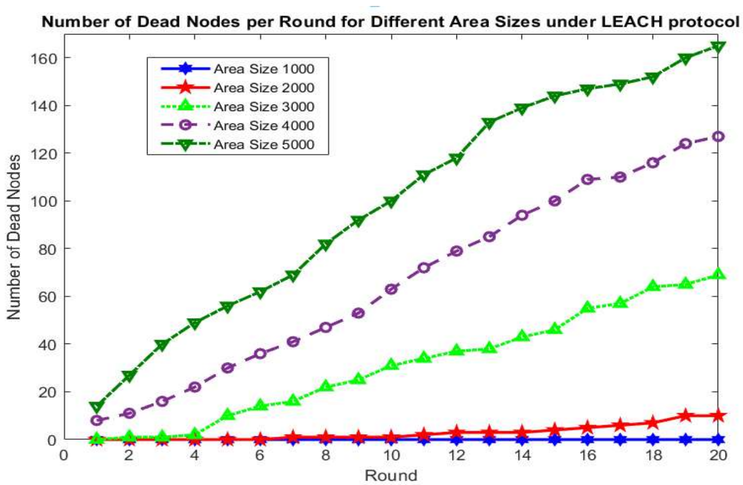


**Figure 31.** Number of Dead Nodes per Round for Different Area Sizes under LEACH Protocol**.**

 doi:10.20944/preprints202603.1394.v1



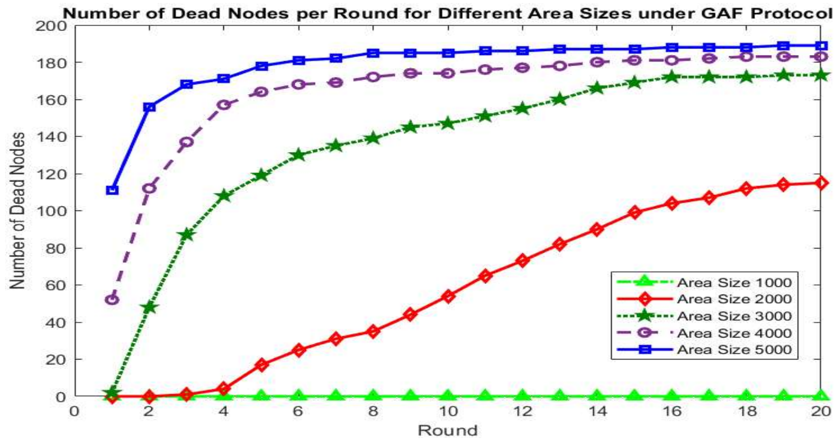


**Figure 32.** Number of Dead Nodes per Round for Different Area Sizes under GAF Protocol**.**

Figure 33 compares the performance of four distinct protocols LEACH, PEBAIS, TEEN, and GAF regarding the number of inactive nodes per round within a set area of 1000 meters. The GAF protocol exhibits the most accelerated rise in deceased nodes, with node mortality commencing about round 30 and surging dramatically, culminating in over 18 dead nodes by round 60. Conversely, the other protocols- LEACH, PEBAIS, and TEEN- demonstrate far superior energy efficiency within this particular area size, resulting in minimal to no node fatalities until the final rounds. PEBAIS and TEEN have a nearly horizontal trajectory, with no substantial rise in dead nodes until subsequent to round 50. LEACH exhibits a comparable pattern, with node fatalities commencing solely in the latter rounds. Figure 34 compares LEACH, PEBAIS, TEEN, and GAF inactive nodes each round in a 2000-meter area. GAF has the fastest node death escalation, starting at round 10 and reaching over 150 by round 60. TEEN and PEBAIS perform similarly, with a more constant increase in dead nodes, reaching 110 by simulation's end. LEACH has the slowest node mortality increase, reaching 90 nodes by 60. In medium-sized regions, GAF depletes node energy faster, reducing network lifespan, while LEACH's energy-efficient clustering and communication techniques extend network lifespan. PEBAIS and TEEN successfully extend network longevity, while LEACH outperforms them in this area size. Figure 35 compares dead nodes over rounds for LEACH, PEBAIS, TEEN, and GAF procedures in a 4000-meter area. GAF had the deadest nodes, 160 at the 20th round, indicating higher energy usage. TEEN and PEBAIS stabilise at 150 dead nodes by the 20th round, conserving somewhat more energy than GAF. LEACH routinely outperforms other procedures, reducing node mortality and ending with 130 inactive nodes by the 20th round. GAF consumes more energy, while LEACH is more energy efficient in medium-to-large areas, increasing network lifespan better than other protocols. Figure 36 shows 25 rounds of dead node tracking for LEACH, PEBAIS, TEEN, and GAF in a 5000-meter area. GAF performs worst, with roughly 180 dead nodes by the 10th round, showing it consumes the most energy in large areas. TEEN stabilises around 170 dead nodes after 15 rounds, like PEBAIS. LEACH has a slower rise in dead nodes, ending at 150, indicating better energy efficiency and a longer network lifespan in large regions. GAF accelerates node energy depletion in large-area wireless sensor networks, although LEACH conserves energy better. LEACH, PEBAIS, TEEN, and GAF network lifetime per round in a 5000-meter area is shown in Figure 37. LEACH has the longest network lifespan, decreasing from 28 to 24 rounds at the end. Durable networks and efficient energy management are indicated. PEBAIS, TEEN, and GAF have comparable tendencies but more erraticism; their network lifetimes range from 14 to 20 cycles. GAF has the most variability compared to PEBAIS and TEEN, but it stabilises at 18 rounds, indicating a little better energy balance. The huge difference between LEACH and TEEN and PEBAIS highlights its usefulness in optimising network lifespan in large installations. LEACH, PEBAIS, TEEN, and GAF procedures' signal-to-noise ratio (SNR) per round in 5000 meters is compared in Figure 38. GAF maintains a consistent SNR approximately 14 dB throughout the simulation, proving signal integrity. In some rounds, LEACH

Preprints.org (www.preprints.org) | NOT PEER-REVIEWED | Posted: 18 March 2026 doi:10.20944/preprints202603.1394.v1



may maintain higher SNR, but its fluctuations signal less consistent performance. Its max. is 17 dB. PEBAIS and TEEN have the lowest SNR values (8–12 dB), indicating poorer communication than GAF and LEACH. GAF's consistent SNR predicts higher signal quality in large-scale networks, while the other protocols' unpredictability and lower SNR suggest communication issues under similar situations. Figure 39 illustrates a comparative assessment of energy usage per round for the LEACH, PEBAIS, TEEN, and GAF protocols within a wireless sensor network over an area of 5000 meters. The GAF protocol has the highest stability and minimal energy usage, constantly remaining below 200 units across all rounds, establishing it as the most energy-efficient protocol in this context. LEACH also exhibits consistently low and stable energy consumption, however with modest variations. Conversely, PEBAIS and TEEN demonstrate significant fluctuations in energy consumption, with PEBAIS surging beyond 1200 units in specific rounds and TEEN attaining such elevated amounts sporadically. The increases in PEBAIS and TEEN indicate suboptimal energy utilisation, likely resulting from elevated communication overheads and increased node activity during particular rounds. The investigation reveals that GAF excels in energy conservation, succeeded by LEACH, whereas PEBAIS and TEEN exhibit elevated and more erratic energy use, potentially affecting network longevity.

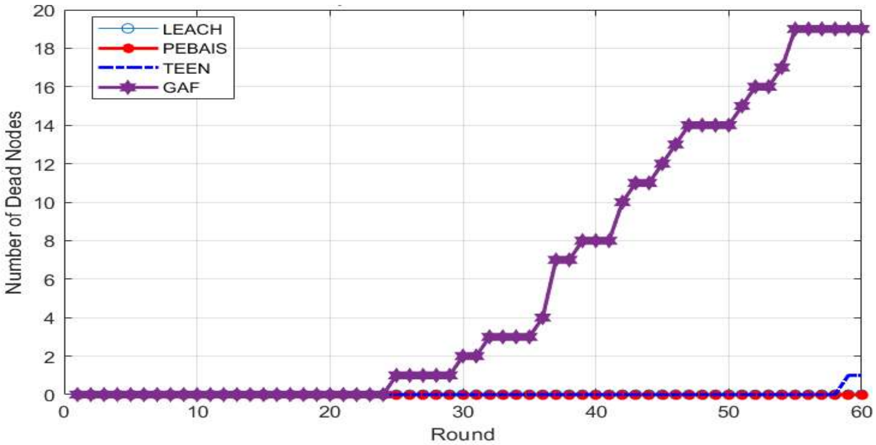


**Figure 33.** Number of Dead Nodes per Round for Different Protocols for Area Size = 1000.

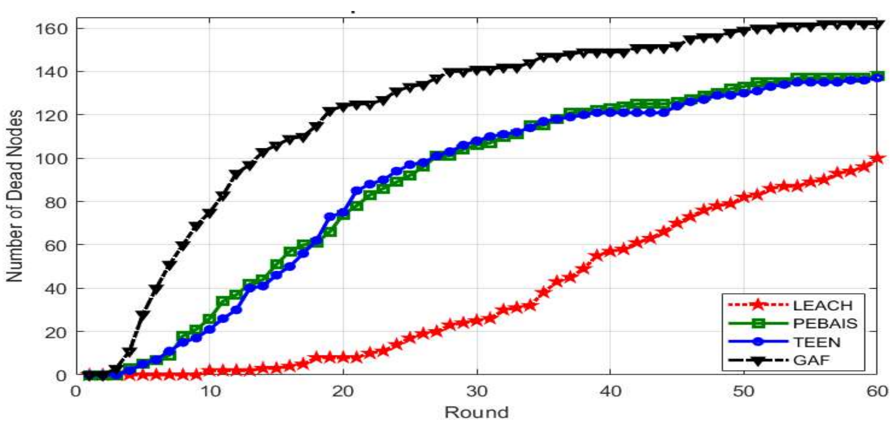


**Figure 34.** Number of Dead Nodes per Round for Different Protocols for Area = 2000.

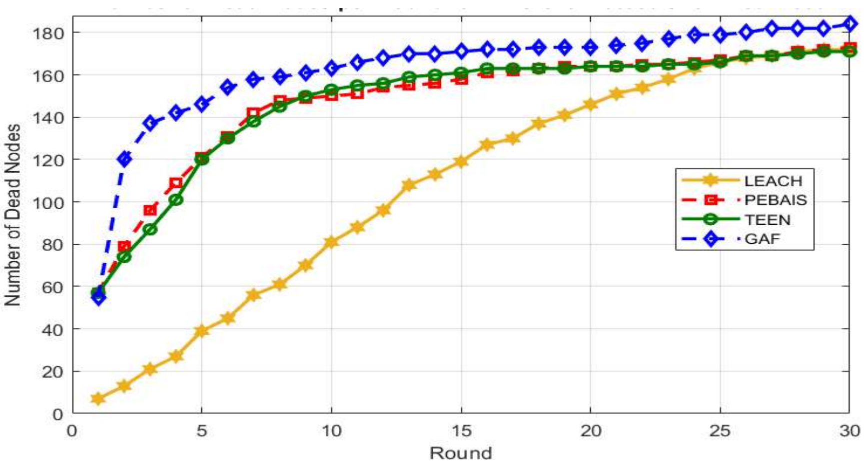


**Figure 35.** Number of Dead Nodes per Round for Different Protocols for Area = 4000.

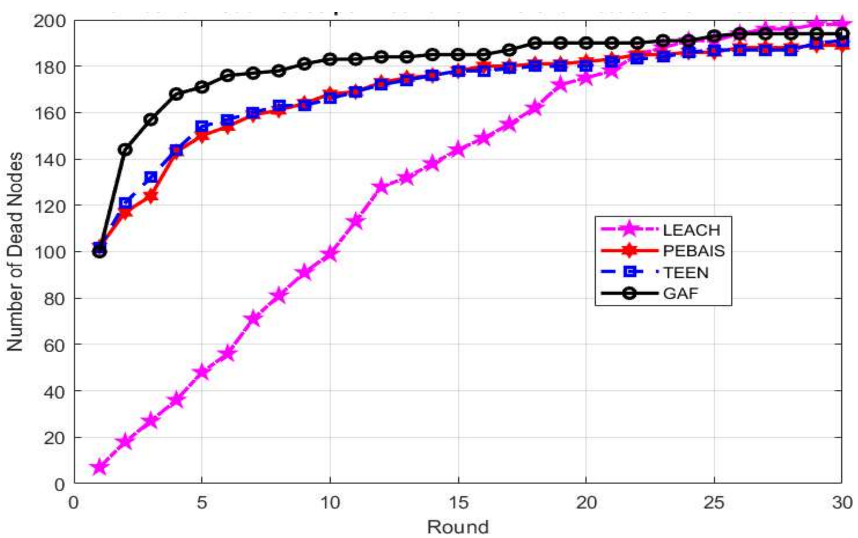


**Figure 36.** Number of Dead Nodes per Round for Different Protocols for Area = 5000.

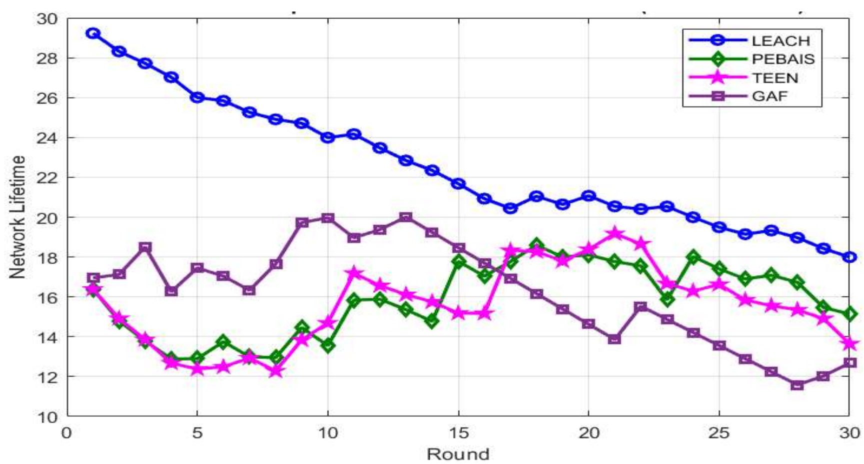


**Figure 37.** Network Lifetime per Round for Different Protocols (Area Size 5000).

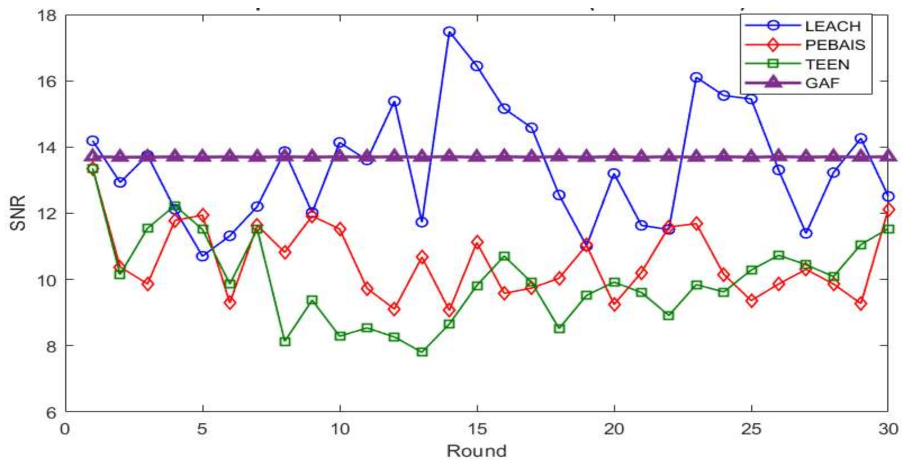


**Figure 38.** SNR per Round for Different Protocols (Area Size 5000).

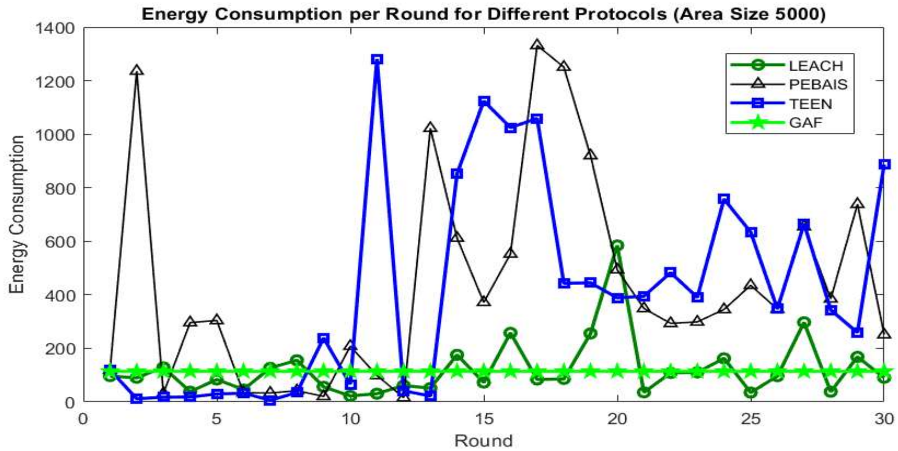


**Figure 39.** Energy Consumption per Round for Different Protocols (Area Size 5000).

In a 5000-meter wireless sensor network, Figure 40 illustrates latency per round for the LEACH, PEBAIS, TEEN, and GAF protocols. Initially, latency rises quickly for all protocols, with TEEN experiencing the most significant increase. However, all protocols stabilize around 1.8 seconds, with LEACH maintaining slightly lower latency throughout the rounds, demonstrating a minor advantage in communication delay. GAF and PEBAIS show similar latency patterns, and the consistent performance across rounds indicates reliable latency management for large network areas, positioning LEACH as the most efficient in reducing delays. In Figure 41, throughput per round is shown for the same four protocols. Throughput increases in the initial rounds, particularly for TEEN, and then stabilizes around 180–190 bps by round 5. GAF consistently achieves the highest throughput, with PEBAIS and TEEN following closely, while LEACH has slightly lower performance. Overall, GAF maintains a marginal advantage in data transfer rates, making it most effective in sustaining high throughput among the four protocols. Figure 42, illustrates the variation in Bit Error Rate (BER) for the four protocols LEACH, PEBAIS, TEEN, and GAF over multiple simulation rounds. The BER values remain consistently low, ranging between 0 and 0.01, indicating reliable network performance with occasional errors. GAF and PEBAIS demonstrate more frequent and pronounced spikes, suggesting potential instability in communication reliability during certain rounds. In contrast, LEACH and TEEN exhibit relatively stable BER trends across the rounds.

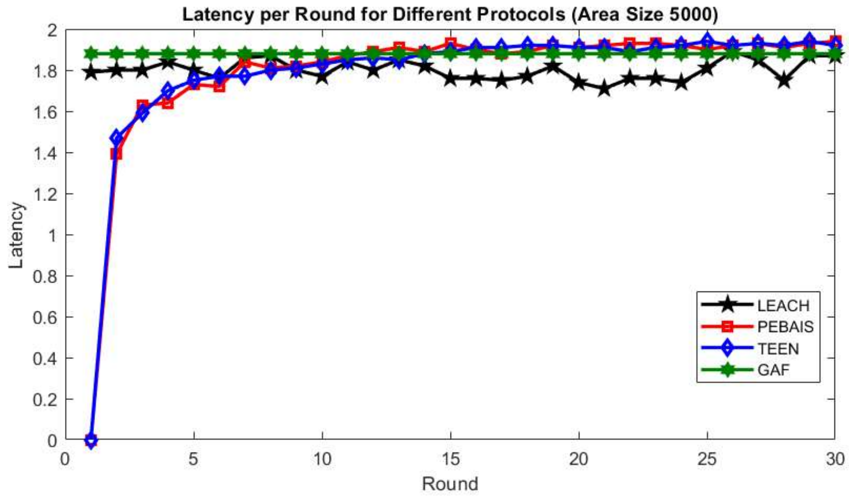


**Figure 40.** Latency per Round for Different Protocols (Area Size 5000).

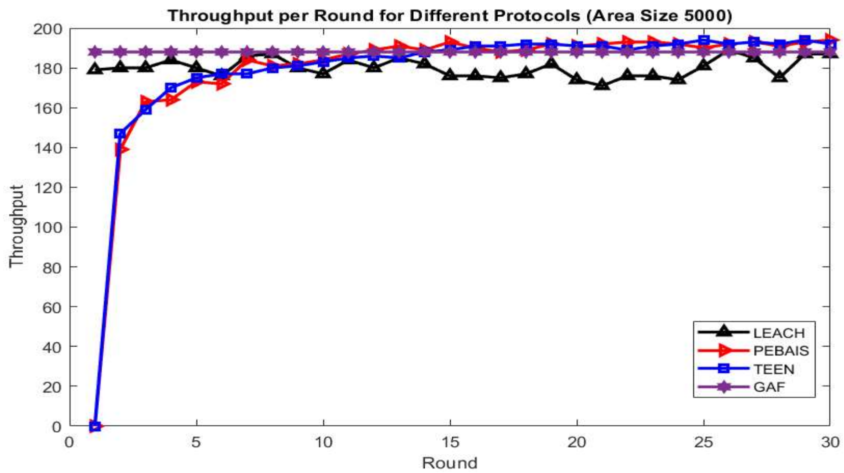


**Figure 41.** Throughput per Round for Different Protocols (Area Size 5000).

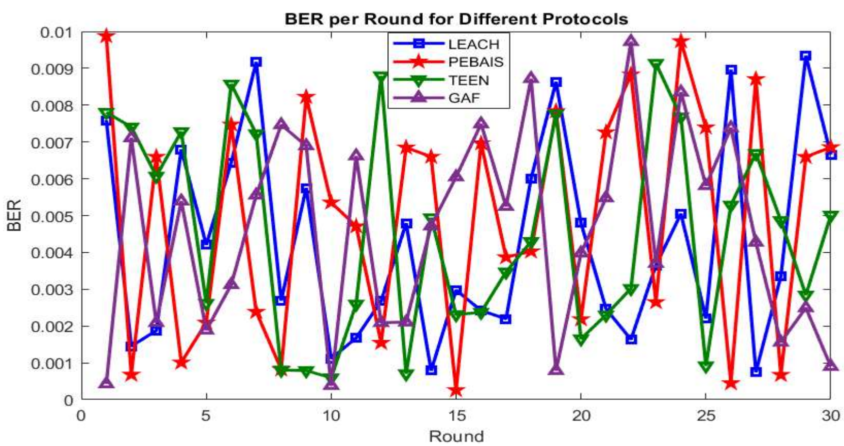


**Figure 42.** BER Comparison Across Rounds for Different Protocols.

## 5. Conclusions

The contribution of the present study involves an in-depth review of different WSN communication protocols suited for radioactive environments. We focused on four protocols: **Low-**

**Energy Adaptive Clustering Hierarchy (LEACH)**, **Power-Efficient and Balanced Aggregation in Sensor Networks (PEBAIS)**, **Threshold-sensitive Energy Efficient Network (TEEN)**, and **Geographic Adaptive Fidelity (GAF)**. Extensive simulations were conducted involving 200 sensor nodes over ten rounds to analyze the performance of these protocols under realistic conditions. Simulations were designed with parameters such as an area size of 5000 $m^2$, initial node energy of 0.5 Joules, and a data packet size of 4000 bits, with an energy consumption of $50x10^{-9}$ Joules per bit.

The results reveal the distinct advantages and limitations of each protocol:

- LEACH demonstrated effective cluster formation and data aggregation, maintaining consistent throughput and low bit error rates. However, it exhibited significant fluctuations in energy consumption and latency, particularly in the initial rounds, which impacted the overall network lifetime and response times.
- PEBAIS showed superior energy management, stabilizing energy consumption after the initial rounds and maintaining zero-bit error rates throughout the simulation. Its latency stabilized at around 2 seconds, and throughput remained consistent at approximately 200 bits per second, demonstrating its efficiency in reliable data transfer. The SNR in PEBAIS fluctuated between 12 and 16 dB, indicating challenges in maintaining high-quality signal transmission, although it generally outperformed LEACH in this aspect.
- TEEN, being designed for reactive networks, excelled in scenarios requiring event-based data transmission. By transmitting data only when certain thresholds were exceeded, TEEN minimized energy consumption significantly while ensuring timely responses to critical events. However, its performance was sensitive to threshold parameter settings, which required careful optimization to achieve a balance between responsiveness and energy efficiency.
- GAF, leveraging geographic location information, demonstrated energy conservation by turning off redundant nodes while maintaining routing fidelity. This approach proved particularly effective in extending network lifetime, especially in scenarios with sparse node deployment. However, GAF's reliance on location information occasionally introduced latency in scenarios where rapid data transmission was required.

The **Network Lifetime** metrics highlighted the robustness of PEBAIS and GAF, both exhibiting prolonged operational periods due to their energy-efficient mechanisms. TEEN performed well in event-driven scenarios, ensuring rapid and reliable responses with minimal energy use, while LEACH, despite its efficiency in cluster formation, lagged in sustaining network operations over extended periods. The novelty of this work lies in its detailed and realistic evaluation of multiple communication protocols under conditions specific to radioactive environments. By incorporating advanced metrics such as SNR, BER, and energy consumption, this study provides a comprehensive understanding of protocol performance directly applicable to the nuclear industry. These findings underscore the potential of WSNs in hazardous environments, where improved protocols for energy management and data integrity directly translate to enhanced safety, reduced operational costs, and reliable environmental monitoring. In addition, **PEBAIS** and **GAF** emerged as robust options for sustaining network operations, while **TEEN** proved ideal for critical event-driven monitoring. Future work should explore hybrid models that integrate the strengths of these protocols to further enhance the resilience and efficiency of WSNs in challenging environments. These findings provide a valuable framework for the development and optimization of WSNs, contributing to more effective and sustainable monitoring solutions in the field of environmental radiation detection.

**Funding:** This research received no external funding.

**Data Availability Statement:** The original contributions presented in this study are included in the article. Further inquiries can be directed to the corresponding author(s).

**Acknowledgments:** This work has been supported by the IAEA, Vienna, Austria, under the framework of the IAEA Coordinated Research Project Number J02020: Nuclear Forensics Science to Bridge the Radiological Crime Scenes to the Nuclear Forensics Laboratory. This support has been instrumental in advancing the research on

energy-efficient wireless sensor network protocols tailored for radioactive environments, contributing to improved monitoring and safety mechanisms in critical applications.

**Conflicts of Interest:** The authors declare no conflict of interest.

## References


1. Liu, N.; Wang, J.; Tao, F.; Fu, Z.; Liu, B., EDRP-GTDQN: An adaptive routing protocol for energy and delay optimization in wireless sensor networks using game theory and deep reinforcement learning. Ad Hoc *Networks* **2025,** 166, 103687.
2. Akkaya, K.; Younis, M., A survey on routing protocols for wireless sensor networks. Ad Hoc *Networks* **2005,** 3, (3), 325-349.
3. Ali, E. H.; Sheta, A. A.; El-Araby, S. M.; Mahmoud, M. I.; Mahmoud, T. A., A self-organized fuzzy neural model for the pressurizer system in nuclear power plants. *Annals of Nuclear Energy* **2026,** 227, 111947.
4. Kaur, P.; Singh, G.; Kaur, P., Intellectual detection and validation of automated mammogram breast cancer images by multi-class SVM using deep learning classification. *Informatics in Medicine Unlocked* **2019,** 16, 100239.
5. Fanian, F.; Kuchaki Rafsanjani, M., Cluster-based routing protocols in wireless sensor networks: A survey based on methodology. *Journal of Network and Computer Applications* **2019,** 142, 111-142.
6. Mahmoud, T. A.; Sheta, A. A.; Fikry, R. M.; Ali, E. H.; El-araby, S. M.; Mahmoud, M. I., Design of data-driven model for the pressurizer system in nuclear power plants using a TSK fuzzy neural network. *Nuclear Engineering and Design* **2022,** 399, (April), 112015-112015.
7. Daanoune, I.; Abdennaceur, B.; Ballouk, A., A comprehensive survey on LEACH-based clustering routing protocols in Wireless Sensor Networks. Ad Hoc *Networks* **2021,** 114, 102409.
8. Singh, S. P.; Sharma, S. C., A Survey on Cluster Based Routing Protocols in Wireless Sensor Networks. *Procedia Computer Science* **2015,** 45, 687-695.
9. Sheta, A. A.; Ali, E. H.; Fikry, R. M.; Mahmoud, T. A.; El-Araby, S. M.; Mahmoud, M. I., Processor-in-the-Loop Simulation and Multivariable Control System Design for Pressurizer System in Nuclear Power Plants. *Arabian Journal for Science and Engineering* **2025**.
10. El_Tokhy, M. S.; Rozovs, S.; Lubashevskiy, A.; Kasban, H.; Ali, E. H., Optimization of dead time correction for digital gamma ray spectroscopy based on social spider algorithm. *Nuclear Analysis* **2025,** 4, (3), 100183.
11. Raj, V. P.; Duraipandian, M., An energy-efficient cross-layer-based opportunistic routing protocol and partially informed sparse autoencoder for data transfer in wireless sensor network. *Journal of Engineering Research* **2024,** 12, (1), 122-132.
12. Harihara Gopalan, S.; Takale, D. G.; Jayaprakash, B.; Pandiya Raj, V., An energy efficient routing protocol with fuzzy neural networks in wireless sensor network. *Ain Shams Engineering Journal* **2024,** 15, (10), 102979.
13. Saleem, K.; Wang, L.; Bharany, S., Survey of AI-driven routing protocols in underwater acoustic networks for enhanced communication efficiency. *Ocean Engineering* **2024,** 314, 119606.
14. Roberts, M. K.; Thangavel, J.; Aldawsari, H., An improved dual-phased meta-heuristic optimization-based framework for energy efficient cluster-based routing in wireless sensor networks. *Alexandria Engineering Journal* **2024,** 101, 306-317.
15. U, N. N.; A, M.; C, V.; R, D., A score based link delay aware routing protocol to improve energy optimization in wireless sensor network. *Journal of Engineering Research* **2023,** 11, (4), 404-413.
16. Omondi, G.; Olwal, T. O., Towards artificial intelligence-aided MIMO detection for 6G communication systems: A review of current trends, challenges and future directions. *e-Prime - Advances in Electrical Engineering, Electronics and Energy* **2023,** 6, 100376.
17. din, N. M. u.; Dar, R. A.; Rasool, M.; Assad, A., Breast cancer detection using deep learning: Datasets, methods, and challenges ahead. *Computers in Biology and Medicine* **2022,** 149, 106073.
18. Guo, W.; Zhang, W., A survey on intelligent routing protocols in wireless sensor networks. *Journal of Network and Computer Applications* **2014,** 38, 185-201.
19. Ali, E. H.; El-Tokhy, M. S.; Kayed, S., Outage Probability and Capacity improvement of A Wireless Communication Systems. *Arab Journal of Nuclear Sciences and Applications* **2023,** 0, (0), 0-0.

20. Habash, M. Y.; Ayad, N.; Ammar, A. E. A., A Framework for Event Detection in Nuclear Facilities Using Wireless Sensors and Actors Networks. *Nuclear Technology* **2022,** 208, 1484-1495.
21. Chithaluru, P. K.; Khan, M. S.; Kumar, M.; Stephan, T., ETH-LEACH: An energy enhanced threshold routing protocol for WSNs. *International Journal of Communication Systems* **2021,** 34, (12).
22. Hajipour, Z.; Barati, H., EELRP: energy efficient layered routing protocol in wireless sensor networks. *Computing* **2021,** 103, (12), 2789-2809.
23. Vinitha, A.; Rukmini, M. S. S.; Dhirajsunehra, Secure and energy aware multi-hop routing protocol in WSN using Taylor-based hybrid optimization algorithm. *Journal of King Saud University - Computer and Information Sciences* **2022,** 34, (5), 1857-1868.
24. Xu, C.; Xiong, Z.; Zhao, G.; Yu, S., An Energy-Efficient Region Source Routing Protocol for Lifetime Maximization in WSN. *IEEE Access* **2019,** 7, 135277-135289.
25. Ding, Z.; Shen, L.; Chen, H.; Yan, F.; Ansari, N., Energy-Efficient Relay-Selection-Based Dynamic Routing Algorithm for IoT-Oriented Software-Defined WSNs. *IEEE Internet of Things Journal* **2020,** 7, (9), 9050-9065.
26. Zhang, Y.; Ren, Q.; Song, K.; Liu, Y.; Zhang, T.; Qian, Y., An Energy-Efficient Multilevel Secure Routing Protocol in IoT Networks. *IEEE Internet of Things Journal* **2022,** 9, (13), 10539-10553.
27. Ahmed Elsmany, E. F.; Omar, M. A.; Wan, T.-C.; Altahir, A. A., EESRA: Energy Efficient Scalable Routing Algorithm for Wireless Sensor Networks. *IEEE Access* **2019,** 7, 96974-96983.
28. Zhang, W.; Liu, Y.; Han, G.; Feng, Y.; Zhao, Y., An Energy Efficient and QoS Aware Routing Algorithm Based on Data Classification for Industrial Wireless Sensor Networks. *IEEE Access* **2018,** 6, 46495-46504.
29. Yun, W.-K.; Yoo, S.-J., Q-Learning-Based Data-Aggregation-Aware Energy-Efficient Routing Protocol for Wireless Sensor Networks. *IEEE Access* **2021,** 9, 10737-10750.
30. Fang, W.; Zhang, W.; Yang, W.; Li, Z.; Gao, W.; Yang, Y., Trust management-based and energy efficient hierarchical routing protocol in wireless sensor networks. *Digital Communications and Networks* **2021,** 7, (4), 470-478.
31. Zhang, W.; Li, L.; Han, G.; Zhang, L., E2HRC: An Energy-Efficient Heterogeneous Ring Clustering Routing Protocol for Wireless Sensor Networks. *IEEE Access* **2017,** 5, 1702-1713.
32. Ding, F.; Song, G.; Yin, K.; Li, J.; Song, A., A GPS-enabled wireless sensor network for monitoring radioactive materials. *Sensors and Actuators A: Physical* **2009,** 155, (1), 210-215.
33. Shafei, M. A. R.; Ibrahim, D. K.; Bahaa, M., Application of PSO tuned fuzzy logic controller for LFC of two-area power system with redox flow battery and PV solar park. *Ain Shams Engineering Journal* **2022,** 13, (5), 101710.
34. Mountrakis, G.; Heydari, S. S., Harvesting the Landsat archive for land cover land use classification using deep neural networks: Comparison with traditional classifiers and multi-sensor benefits. *ISPRS Journal of Photogrammetry and Remote Sensing* **2023,** 200, 106-119.
35. Isaac, A.; Nehemiah, H. K.; Dunston, S. D.; Elgin Christo, V. R.; Kannan, A., Feature selection using competitive coevolution of bio-inspired algorithms for the diagnosis of pulmonary emphysema. *Biomedical Signal Processing and Control* **2022,** 72, 103340.
36. Gavali, A.; Vaze, V.; Ubale, S., Energy optimization using swarm intelligence for IoT-authorized underwater wireless sensor networks. *Microprocessors and Microsystems* **2021**.
37. Sheta, A. A.; Ali, E. H.; Fikry, R. M.; ElAraby, S. M.; Mahmoud, T. A.; Mahmoud, M. I., A developed analytical model for the pressurizer unit in nuclear power plants. *Journal of Radiation Research and Applied Sciences* **2021,** 14, (1), 179-203.
38. H. Kasban, E. H. A., Mohamed S. EL-Tokhy and H. Arafa, Improvement of Radiotracer Residence Time Distribution Analysis in Industrial Applications. *International Journal of System Signal Control and Engineering Application* **2021,** 14, (1), 1-17.
39. Kasban, H.; Ali, E. H.; Arafa, H., Diagnosing Plant Pipeline System Performance Using Radiotracer Techniques. *Nuclear Engineering and Technology* **2017,** 49, (1), 196-208.
40. Wang, Z.; Xu, D., Online optimization of intelligent reflecting surface-aided energy-efficient IoT-edge computing. *Future Generation Computer Systems* **2023,** 141, 611-625.

41. Manjeshwar, A.; Agrawal, D. P. In *TEEN: a routing protocol for enhanced efficiency in wireless sensor networks*, Proceedings 15th International Parallel and Distributed Processing Symposium. IPDPS 2001, 23-27 April 2001, 2001; 2001; pp 2009-2015.
42. Kumar, V. K.; Khunteta, A. In *Energy Efficient PEGASIS Routing Protocol for Wireless Sensor Networks*, 2018 2nd International Conference on Micro-Electronics and Telecommunication Engineering (ICMETE), 20-21 Sept. 2018, 2018; 2018; pp 91-95.
43. Korpeoglu, I.; Tan, H., Power efficient data gathering and aggregation in wireless sensor networks. *ACM SIGMOD Record* **2003,** 32, 66-71.
44. Chandel, A.; Chouhan, V. S.; Sharma, S. In *A Survey on Routing Protocols for Wireless Sensor Networks*, Advances in Information Communication Technology and Computing, Singapore, 2021//, 2021; Goar, V.; Kuri, M.; Kumar, R.; Senjyu, T., Eds. Springer Singapore: Singapore, 2021; pp 143-164.
45. Xu, Y.; Heidemann, J.; Estrin, D., Geography-informed energy conservation for Ad Hoc routing. In *Proceedings of the 7th annual international conference on Mobile computing and networking*, ACM: 2001.
46. Affane M, A. R.; Satori, H., Machine learning attack detection based-on stochastic classifier methods for enhancing of routing security in wireless sensor networks. Ad Hoc *Networks* **2024,** 163, 103581.
47. Lalle, Y.; Fourati, M.; Fourati, L. C.; Barraca, J. P., Communication technologies for Smart Water Grid applications: Overview, opportunities, and research directions. *Computer Networks* **2021,** 190, 107940.
48. Ghosh, S.; Talapatra, S.; Sharma, J.; Chatterjee, N.; Rahaman, H.; Maity, S. P., Dual Mode VLSI Architecture for Spread Spectrum Image Watermarking using Binary Watermark. *Procedia Technology* **2012,** 6, 784-791.
49. Bucci, G.; Fiorucci, E.; Landi, C.; Ocera, G., Architecture of a digital wireless data communication network for distributed sensor applications. *Measurement* **2004,** 35, (1), 33-45.
50. Suryadevara, N. K., Energy and latency reductions at the fog gateway using a machine learning classifier. *Sustainable Computing: Informatics and Systems* **2021,** 31, 100582.
51. Zenia, N. Z.; Aseeri, M.; Ahmed, M. R.; Chowdhury, Z. I.; Shamim Kaiser, M., Energy-efficiency and reliability in MAC and routing protocols for underwater wireless sensor network: A survey. *Journal of Network and Computer Applications* **2016,** 71, 72-85.
52. El-Tokhy, M. S.; Ali, E. H.; Kasban, H., Performance Improvement of OFDMA Systems Through Wireless Communication Channels. *Wireless Personal Communications* **2022,** 124, (3), 2447-2473.
53. Islam, K. Y.; Ahmad, I.; Habibi, D.; Waqar, A., A survey on energy efficiency in underwater wireless communications. *Journal of Network and Computer Applications* **2022,** 198, 103295.
54. Elrefaei, J. H.; Kunber, H.; Shaat, M. K.; Madian, A. H.; Saad, M. H., Energy-efficient wireless sensor network for nuclear radiation detection. *Journal of Radiation Research and Applied Sciences* **2019,** 12, (1), 1-9.
55. Okdem, S., A cross-layer adaptive mechanism for low-power wireless personal area networks. *Computer Communications* **2016,** 78, 16-27.
56. Venugopal, D.; Mohan, S.; Raja, S., An efficient block based lossless compression of medical images. *Optik* **2016,** 127, (2), 754-758.
57. Wang, R.; Song, C.; Gao, M.; Zhao, J.; Xu, Z., Model-data fusion domain adaptation for battery State of Health estimation with fewer data and simplified feature extractor. *Journal of Energy Storage* **2023,** 60, 106686.
58. Luca, R.; Whiteley, M.; Neville, T.; Shearing, P. R.; Brett, D. J. L., Comparative study of energy management systems for a hybrid fuel cell electric vehicle - A novel mutative fuzzy logic controller to prolong fuel cell lifetime. *International Journal of Hydrogen Energy* **2022,** 47, (57), 24042-24058.
59. Ahmed, M.; Salleh, M.; Channa, M. I., Routing protocols based on protocol operations for underwater wireless sensor network: A survey. *Egyptian Informatics Journal* **2018,** 19, (1), 57-62.
60. Abdou, M.; Amer, H. M.; Abdelsalam, M. M.; Khalil, A. T., EVRP: A novel geometrical based energy efficient eye vision routing protocol for wireless sensor networks based on the k-means algorithm. Ad Hoc *Networks* **2024,** 160, 103528.
61. Saemi, B.; Goodarzian, F., Energy-efficient routing protocol for underwater wireless sensor networks using a hybrid metaheuristic algorithm. *Engineering Applications of Artificial Intelligence* **2024,** 133, 108132.

doi:10.20944/preprints202603.1394.v1



**Disclaimer/Publisher's Note:** The statements, opinions and data contained in all publications are solely those of the individual author(s) and contributor(s) and not of MDPI and/or the editor(s). MDPI and/or the editor(s) disclaim responsibility for any injury to people or property resulting from any ideas, methods, instructions or products referred to in the content.